

COMPUTER SIMULATION OF LAMINAR FORCED CONVECTIVE HEAT
TRANSFER IN THE ENTRANCE REGION OF A STRAIGHT
CHANNEL FOR CONSTANT- AND
VARIABLE-PROPERTY GASES

By

MATTHEW JESS MAXWELL
”

Bachelor Science in Mechanical Engineering

Oklahoma State University

Stillwater, Oklahoma

1983

Submitted to the Faculty of the Graduate College
of the Oklahoma State University
in partial fulfillment of the requirements
for the Degree of
MASTER OF SCIENCE
May, 1985

Thesis
1985
M465c
cop. 2



COMPUTER SIMULATION OF LAMINAR FORCED CONVECTIVE HEAT
TRANSFER IN THE ENTRANCE REGION OF A STRAIGHT
CHANNEL FOR CONSTANT- AND
VARIABLE-PROPERTY GASES

Thesis Approved:

A. J. Ghajar

Thesis Adviser

F. O. Thomas

Donald G. Riley

Norman N. Duncan

Dean of Graduate College

PREFACE

I wish to thank the Faculty members at Oklahoma State University who have contributed to the furthering of my knowledge. Also, my appreciation goes out to Dr. D. G. Lilley for his assistance and guidance in the computational field of my study and Dr. F. O. Thomas for his guidance at the onset of this project.

I am deeply indebted to my adviser, Dr. A. J. Ghajar, whose guidance and inspiration through undergraduate and graduate college has taken me to the height of my education at Oklahoma State University.

My thanks goes to Dr. Y. I. Sharaf-Eldeen, Yousef Zurigat, Sankaron Mohan, and my good friend, Brett Newman, for their assistance and encouragement, and to Mrs. Dee Meier for typing and coordinating the final draft of my thesis.

I must also thank my family and friends for their moral support and encouragement, and to my fiancée, Deanna Senter, for her uplifting love and prayer while I was attending Oklahoma State University.

TABLE OF CONTENTS

Chapter	Page
I. INTRODUCTION	1
1.1 Objectives	2
1.2 Instrument of Study	2
1.3 Review of Previous Investigations	3
II. DEVELOPMENT OF DISCRETIZED EQUATIONS AND BOUNDARY CONDITIONS	6
2.1 Conservation Equations	6
2.2 General Discretized Equation	8
2.3 Grid Systems and Dependent Variable Locations	17
2.4 Specific Discretized Equations	22
2.5 Implementation of Boundary Conditions	25
2.6 Summary	31
III. VARIABLE-PROPERTY METHOD	33
3.1 Reference Temperature and Property Ratio Methods	33
3.2 Thermo-Physical-Property Update Method	35
3.3 Summary	36
IV. NUMERICAL STUDY OF LAMINAR FORCED CONVECTION HEAT TRANSFER IN THE ENTRANCE REGION OF A FLAT DUCT	39
4.1 Results of Constant-Property Model	41
4.2 Results of Variable-Property Model	47
4.3 Variable Property Effects	53
4.4 Summary	62
V. SUMMARY, CONCLUSIONS, AND RECOMMENDATIONS	63
5.1 Summary and Conclusions	63
5.2 Recommendations	64
BIBLIOGRAPHY	66
APPENDIX A - FLOW CHART FOR COMPUTER CODE	68
APPENDIX B - LISTING OF COMPUTER CODE FOR VARIABLE- PROPERTY MODEL	70

LIST OF TABLES

Table	Page
I. Local Flow Evaluation and Neighboring Influence for Limiting Values of Pe	12
II. Mean and Maximum Percent Deviations for Property- Equations of air Evaluated at Standard Atmospheric Pressure	37
III. Percent Difference In Nu_x Between Constant and Variable-Property Solutions	57

LIST OF FIGURES

Figure	Page
1. Control Volume for the Two-Dimensional Axisymmetric Domain	10
2. Two-Dimensional Axisymmetric Grid System	18
3. Perspective View of P-CELL	18
4. u-Grid System	19
5. v-Grid System	20
6. u- and v-Velocity Subscript Definition	21
7. Northern Boundary	26
8. Northern Boundary With Near Boundary P-CELL	28
9. Geometry of Problem	42
10. Comparison of Constant-Property Results with [3] for $Re_d = 20$	45
11. Comparison of Constant-Property Results with [3] for $Re_d = 1000$	46
12. Comparison of Variable-Property Model with Experimental Results of [4] at $Re_{de} = 682$	49
13. Comparison of Variable-Property Model with Experimental Results of [4] at $Re_{de} = 1474$	50
14. Variable-Property Results Shifted by Equation (4.14) with Various Inlet Temperatures	51
15. Constant- and Variable-Property Predictions of Nu_x at $T_w = 330.0^{\circ}K$	54
16. Constant- and Variable-Property Predictions of Nu_x at $T_w = 700^{\circ}K$	55
17. Constant- and Variable-Property Predictions of Nu_x at $T_w = 1000^{\circ}K$	56

Figure	Page
18. The Effect of Viscosity Variations on Nu_x for Various Wall-to-Inlet Temperature Ratios	58
19. The Effect of Density Variation on Nu_x for Various Wall-to-Inlet Temperature Ratios	59
20. The Effect of Thermal Conductivity Variations on Nu_x for Various Wall-to-Inlet Temperature Ratios	60
21. The Effect of Specific Heat Variations on Nu_x for Various Wall-to-Inlet Temperature Ratios	61
22. Flow Chart for the TEACH Code	69

NOMENCLATURE

English Letter Symbols

- A - dummy variable
- A_c - cross sectional area between parallel plates, defined by Equation (4.10)
- a - coupling coefficient, Chapter II
- a - half-width between parallel plates, defined in Figure 4.9
- B - dummy variable
- C_f - friction factor
- C_p - specific heat at constant pressure
- d - hydraulic diameter, $d=4a$
- h - local heat transfer coefficient
- J - total flux through interfaces
- k - thermal conductivity
- L - length of parallel plates in streamwise direction, defined in Figure 4.9
- L_∞ - fully developed length
- LO - logical function, referring to Larger Of A or B
- m - mass flow across interface
- Nu_x - local Nusselt number, defined by Equations (4.11) and (4.13)
- Nu_{10} - local Nusselt number, defined by Equation (4.12)
- n - exponent used in Equation (3.1)
- P - cell Peclet number, defined by Equation (2.13)

- P - pressure
- Pr - Prandtl number, $Pr = \mu C_p/k$
- Pr_e - entrance Prandtl number
- \dot{q}_w'' - wall heat flux, defined by Equation (4.8)
- R - non-dimensional radial distance, $R = r/d$
- Re_d - Reynolds number based on hydraulic diameter, $Re_d = \rho u d/\mu$
- Re_{de} - Entrance Reynolds number
- r - radial coordinate direction, defined in Figure 3
- r - rectilinear coordinate normal to streamwise coordinate, defined in Figure 9
- S_C - constant source in linearized source, used in Equation (2.7)
- S_p - slope coefficient for linearized source, used in Equation (2.7)
- S_T - general source term for temperature, used in Equation (2.4)
- St - Stanton number
- S_u - general source term for u-velocity, used in Equation (2.2)
- S_r - general source term for v-velocity, used in Equation (2.3)
- T - local temperature
- T_e - inlet temperature
- T_m - mixed mean temperature, defined by Equation (4.9)
- T_w - wall temperature
- U_e - uniform inlet velocity
- u - local streamwise velocity
- V - average velocity, defined by Equation (4.10)
- v - local radial velocity, Chapter II
- v - local velocity normal to streamwise direction, Chapter IV
- x - streamwise coordinate direction, defined in Figures 3 and 9

- X - non-dimensional streamwise coordinate, $X = 4(x/a)/(Re_d Pr)$
- Y - non-dimensional coordinate, used in Equation (4.12)

Greek Letter Symbols

- β - constant source, $\beta = S_c (r_p \Delta x \Delta r)$
- Δ - grid spacing with coordinate direction x or r
- Γ - diffusion coefficient
- ρ - fluid density
- μ - fluid viscosity
- ζ - general dependent variable, $\zeta = u, v, P, T$

Subscripts

- b - evaluated at boundary
- CP - constant property
- E - evaluated at eastern grid point
- e - evaluated at eastern interface
- F - evaluated at a fixed grid point
- N - evaluated at northern grid point
- n - evaluated at northern interface
- P - evaluated at P grid point
- S - evaluated at southern grid point
- s - evaluated at southern interface
- W - evaluated at western grid point
- w - evaluated at western interface
- wall - evaluated at wall
- ζ - for the dependent variable in question

Superscripts

- g - guessed values
- c - corrected values

Abbreviations

- 2-D - Two-dimensional

CHAPTER I

INTRODUCTION

Several numerical studies of laminar forced convection heat transfer for internal flows have appeared in the literature [1-25]. The motivation for such studies has been sparked by a growing interest in the application of compact heat-exchangers where equivalent diameters are small and densities are low (laminar flow). The majority of these studies assume that temperature changes in the thermally developing region are small, and thus the physical properties remain constant throughout this region. In applications such as air cooled nuclear reactors, where parallel plates are used as the medium through which heat is transferred, large temperature differences occur in the entrance region between the plates. These large variations in temperature will affect the physical properties of the fluid, which will in turn affect the development of the inlet velocity and temperature profiles.

Because Prandtl numbers for most gases are near unity, both the velocity and temperature profiles will develop simultaneously when small temperature variations are assumed (i.e., constant physical properties). Regretfully though, when substantial temperature differences occur the variation of properties cause the development of the velocity and temperature profiles to become somewhat irregular. Shumway and McEligot [1] have shown that the physical-property variations associated with most gases will cause reductions in local

heat-transfer coefficients when large temperature gradients are present for air in tube annuli. Therefore, when modeling internal, forced convective heat transfer of gases ($Pr \approx 1$) subjected to large temperature gradients the changes in physical properties of the fluid must be accounted for.

1.1 Objectives

The objectives of this study are:

1. To use an existing code (TEACH (Teaching Elliptic Axisymmetric Characteristics Heuristically) [2]) as an instrument to study two-dimensional laminar forced convective heat transfer in the entrance region of a flat duct (see Chapter II).
2. To check the validity of the constant-property model results with those numerical results obtained by [3] and [4] (see Section 4.1).
3. To incorporate temperature-dependent physical-property relations into the TEACH code to obtain a variable-property model (see Chapter III).
4. To check the validity of the variable-property model with available experimental data (see Section 4.2).
5. To show the effects of individual property variations on local non-dimensionalized heat-transfer coefficients (see Section 4.3).

1.2 Instrument of Study

Similar to an experimental apparatus that an engineer might use to carry out some type of investigation, the TEACH code is used in this

study to investigate internal forced convection in the entrance region of a flat duct. The finite difference theory used in constructing such a code is well presented by Patankar [5]. However, due to a lack of information in the literature on implementation of boundary conditions, Chapter II will be devoted to developing the necessary information to understand how boundary conditions are incorporated in the TEACH computer program. A generalized flow chart may be found in Appendix A. The FORTRAN code used to model the variable-property model presented in Chapter IV is listed in Appendix B.

1.3 Review of Previous Investigations

As mentioned previously, many investigators have reported their findings on laminar forced convective heat transfer for internal flows. Kays [6], who began his research in this field in 1955, employed Langhaar's [7] velocity profiles, neglecting the effects of the radial component of velocity, to solve the combined entry length problem for a Prandtl number, Pr , of 0.7 in a circular duct. This neglect of the radial velocity overestimates the local Nusselt numbers, Nu_x , for simultaneously developing velocity and temperature profiles. Goldberg [8] extended Kays work by solving the energy equation for Pr in the range of 0.50 to 5.0.

Ulrichson and Schmidt [9] obtained velocity and temperature profiles for laminar flow in the entrance region of a circular tube for $Pr = 0.7$. The radial velocity component was obtained by using the continuity equation and Langhaar's axial velocity profiles.

Further refinement of the entry length problem came from Hornbeck [10]. Hornbeck employed a finite difference method for constant wall

and constant heat flux boundary conditions with $Pr = 0.7, 2, \text{ and } 5$. Manohar [11], Kakac and Özgü [12] give results from their studies of the nonlinear equations for laminar flow of viscous incompressible fluids. Their velocity profile solutions are used to obtain temperature profiles from the energy equation, under constant wall temperature and also under constant heat flux at the wall.

Approximately the same time that Kays began his investigations of heat transfer in circular pipes, Sparrow [13] was investigating the simultaneous development of velocity and temperature profiles for parallel plate flow. Hawang and Fan [14] solved the combined entrance parallel plate problem by a finite difference analysis of the refined momentum and energy equations in rectilinear coordinates. Mercer et al. [4] also based their analysis on the same refined momentum and energy equations but used the stream function definition to obtain a solution. In addition, Mercer et al. supplemented their analysis with experimental work and showed comparisons of their theoretical and experimental results. Nagrang and Hussain [3] took Hawang and Fan's [14] work one step further by including the effects of transverse momentum and axial conduction.

In 1970 Bankston and McEligot [15] introduced a finite difference solution which included property variations for the combined entrance region of a circular duct. Shumway and McEligot [1] extended the previous work to show significant variations in the properties of air for high heating rates through a tube annuli. The combined entry profiles were found by a finite difference solution of the conservation equations neglecting radial momentum. Variations in properties of [1] were based on an inlet Mach number of 0.01 and are described by the

following equations:

$$\frac{C_p}{C_{p_e}} = \left(\frac{T}{T_e}\right)^{0.095}, \quad \frac{K}{K_e} = \left(\frac{T}{T_e}\right)^{0.0805}, \quad \frac{\mu}{\mu_e} = \left(\frac{T}{T_e}\right)^{0.670}, \quad (1.1)$$

where variables subscripted e are evaluated at the inlet of the tube annuli.

From this review of the literature, it is evident that the combined entry length problem is a fundamental problem in heat transfer and fluid flow. With higher heating rates being imposed in the combined entrance region, in such application as the convective heat transfer from parallel plates in gas cooled nuclear reactors, it is important to properly model property variations of the fluid between the plates. In this study a method for accurately predicting velocity and temperature profiles (which have a direct bearing on local heat transfer coefficients) is developed for forced convective heat transfer flows of variable-property gases in the inlet of a straight channel.

CHAPTER II

DEVELOPMENT OF DISCRETIZED EQUATIONS AND BOUNDARY CONDITIONS

In this chapter the governing two-dimensional axisymmetric equations for heat transfer and fluid flow are presented in Section 2.1. In Section 2.2 the general discretized equation is developed by integration of the general differential equation over a control volume with piecewise functional variations of the dependent variables defined by the Hybrid scheme.

The main u -, and v -grid systems are presented in Section 2.3 to reinforce the development of the specific discretized equations for the dependent variables u , v , P , and T . Sections 2.1 through 2.4 are presented so that the reader will have a better understanding of the boundary condition formulation presented in Section 2.6. Knowledge of how these boundary conditions are applied in the TEACH computer code is necessary if one is to obtain realistic field solutions to the governing differential equation.

2.1 Conservation Equations

The main purpose of the TEACH computer code is to solve two-dimensional axisymmetric laminar flow of Newtonian fluids where viscous dissipation and flow work are negligible. The conservation equations which conform to such flow situations are the:

Continuity Equation

$$\frac{\partial}{\partial x} (\rho r u) + \frac{\partial}{\partial r} (\rho r v) = 0, \quad (2.1)$$

x-Momentum Equation

$$\frac{1}{r} \left[\frac{\partial}{\partial x} (\rho r u^2) + \frac{\partial}{\partial r} (\rho r v u) - \frac{\partial}{\partial x} (r \mu \frac{\partial u}{\partial x}) - \frac{\partial}{\partial r} (r \mu \frac{\partial u}{\partial r}) \right] = - \frac{\partial P}{\partial x} + S_u, \quad (2.2)$$

r-Momentum Equation

$$\frac{1}{r} \left[\frac{\partial}{\partial x} (\rho r u v) + \frac{\partial}{\partial r} (\rho r v^2) - \frac{\partial}{\partial x} (r \mu \frac{\partial v}{\partial x}) - \frac{\partial}{\partial r} (r \mu \frac{\partial v}{\partial r}) \right] - \frac{\mu v}{r^2} = - \frac{\partial P}{\partial r} + S_v, \quad (2.3)$$

Energy Equation

$$\frac{1}{r} \left[\frac{\partial}{\partial x} (\rho r u T) + \frac{\partial}{\partial r} (\rho r v T) - \frac{\partial}{\partial x} (r \frac{k}{C_p} \frac{\partial T}{\partial x}) - \frac{\partial}{\partial r} (r \frac{k}{C_p} \frac{\partial T}{\partial r}) \right] = S_T. \quad (2.4)$$

S_u , S_v , and S_T are the generalized source terms.

The implementation of the conservation equations into the TEACH code is done by generating finite difference equations which in the limit (as the grid mesh is refined) are an excellent representation of the conservation equations. The accuracy of such finite difference schemes are discussed by Patankar [5] and Roache [16]. The finite difference equations may be developed by many different methods. The control-volume approach is the simplest to understand and lends itself to a direct physical interpretation.

For the control-volume formulation to work the domain of interest must be subdivided into a number of non-overlapping control volumes. The control volumes, sometimes referred to as cells, surround grid

points which also occupy the domain of interest. The differential Equations (2.1) through (2.4) are integrated over the aforementioned cells, while piecewise continuous functions define how the dependent variables u , v , P , and T vary between the grid points.

The piecewise "profiles", as referred to by Patankar [5], are used to evaluate the integral relations over a designated control volume. The resulting discretized equations contain the dependent variables for all grid points within the region being considered. The discretized equations are then solved to obtain the grid-point values of the dependent variables. The resulting grid-point values represent the solution to the differential equations, without explicit reference as to the piecewise functional variation of the dependent variables between grid points. The concept of dependent variable variations between grid points will be discussed in Section 2.2 of this chapter.

2.2 General Discretized Equation

The governing differential equations may be represented by a common form given as

$$\frac{1}{r} \left[\frac{\partial}{\partial x} (r J_x) + \frac{\partial}{\partial r} (r J_r) \right] = S_\zeta \quad (2.5)$$

J_x and J_r are the total (convection plus diffusion) fluxes defined by

$$J_x \equiv \rho u \zeta - \Gamma_\zeta \frac{\partial \zeta}{\partial x} \quad (2.6a)$$

$$J_r \equiv \rho v \zeta - \Gamma_\zeta \frac{\partial \zeta}{\partial r} \quad (2.6b)$$

For $\zeta = 1$ and $S_\zeta = 0$, Equation (2.5) reduces to the Continuity Equation (2.1). With ζ equal to u or v , $S_\zeta = -\partial P / \partial x + S_u$ or $S_\zeta = \mu v / r^2 - \partial P / \partial r + S_v$ where $S_u = S_v = 0$, and Γ_ζ set to μ , Equation (2.5) reduces to the

u- or v-Momentum Equations (2.2) or (2.3) respectively. Also, to obtain the Energy Equation (2.4) ζ is set equal to T and Γ_ζ may be represented by μ/Pr or k/Cp . By representing the governing differential equations in this common form a common discretized formula may be developed and implemented into a computer code.

The integration of Equation (2.5) over the control volume shown in Figure 1 would give

$$J_e - J_w + J_n - J_s = (S_c + S_p \zeta_p) r_p \Delta x \Delta r, \quad (2.7)$$

where the source term has been linearized; S_c represents the constant part of S_ζ , while S_p is the coefficient of ζ_p . The total flux through the interface at point e is given as

$$J_e = r_p \Delta r \left[(\rho u \zeta)_e - \left(\Gamma_\zeta \frac{\partial \zeta}{\partial x} \right)_e \right]. \quad (2.8a)$$

Similarly for the other interfaces,

$$J_w = r_p \Delta r \left[(\rho u \zeta)_w - \left(\Gamma_\zeta \frac{\partial \zeta}{\partial x} \right)_w \right], \quad (2.8b)$$

$$J_n = r_n \Delta x \left[(\rho v \zeta)_n - \left(\Gamma_\zeta \frac{\partial \zeta}{\partial r} \right)_n \right], \quad (2.8c)$$

$$J_s = r_s \Delta x \left[(\rho v \zeta)_s - \left(\Gamma_\zeta \frac{\partial \zeta}{\partial r} \right)_s \right]. \quad (2.8d)$$

Similarly, we can integrate Equation (2.5), with $\zeta = 1$ in Equations (2.6a) and (2.6b), (Continuity Equation) over the control volume and obtain

$$m_e - m_w + m_n - m_s = 0 \quad (2.9)$$

where m_e , m_w , m_n , and m_s are the mass flow rates through the faces of the control volume. If ρu at the point e is taken to prevail over the

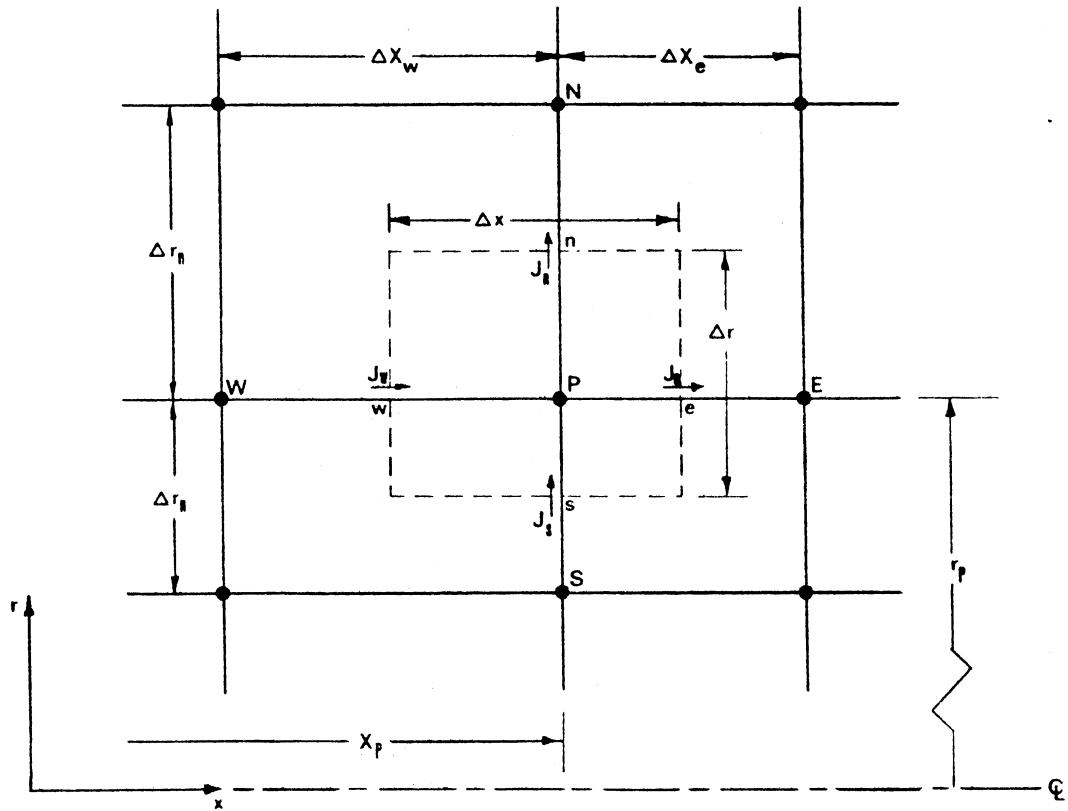


Figure 1. Control Volume for the Two-Dimensional Axisymmetric Domain.

whole interface e, m_e may be represented by

$$m_e = (\rho u)_e r_p \Delta r. \quad (2.10a)$$

Similarly,

$$m_w = (\rho u)_w r_p \Delta r, \quad (2.10b)$$

$$m_n = (\rho v)_n r_n \Delta x, \quad (2.10c)$$

$$m_s = (\rho v)_s r_s \Delta x. \quad (2.10d)$$

By multiplying Equation (2.9) by ζ_p and subtracting it from Equation (2.7), the following relation is obtained:

$$\begin{aligned} & (J_e - m_e \zeta_p) - (J_w - m_w \zeta_p) + (J_n - m_n \zeta_p) \\ & - (J_s - m_s \zeta_p) = (S_c + S_p \zeta_p) r_p \Delta x \Delta r. \end{aligned} \quad (2.11)$$

Expanding the first term in Equation (2.11) gives

$$(J_e - m_e \zeta_p) = r_p \Delta r \left[(\rho u \zeta)_e - \left(\Gamma_\zeta \frac{\partial \zeta}{\partial x} \right)_e \right] - (\rho u)_e r_p \Delta r \zeta_p. \quad (2.12)$$

From Equation (2.12) it can be seen that the discretization of Equation (2.11) may only come about by knowing how ζ varies from point P to point E.

The variation of ζ between any two grid points will depend on the local flow conditions. The grid Peclet number defined by

$$P = \frac{\rho V \Delta}{\Gamma_\zeta}, \quad (2.13)$$

shows the relative strengths of convection and diffusion. With reference to Figure 1, the Peclet number evaluated at e is given by

$$P_e = \frac{(\rho u)_e \Delta x_e}{\Gamma_{\zeta_e}}. \quad (2.13a)$$

For limiting values of the grid Peclet number local evaluations of the flow field may be used to show how ζ is influenced by its neighboring points. Table I gives the evaluation of the local flow field and the influence of the neighboring dependent variables (ζ_E and ζ_p) on ζ_e .

TABLE I
LOCAL FLOW EVALUATION AND NEIGHBORING INFLUENCE FOR
LIMITING VALUES OF Pe

LIMITING CASE	LOCAL FLOW EVALUATION	NEIGHBORS INFLUENCE
$Pe = 0$	$m_e = (\rho u \Delta r)_e$ $r_p = 0$	Total diffusion (or conduction); no convection
$Pe = +\infty$	High convection from West to East	ζ_e largely influenced by upstream (or ζ_p)
$Pe = -\infty$	High convection from East to West	ζ_e largely influenced by upstream (or ζ_E)

For local Peclet numbers near zero a central differencing scheme represents the local functional variation of ζ quite well. But, for $|P| \gg 0$ the central differencing scheme does not satisfactorily predict the influence of neighboring ζ 's. The functional variation of the dependent variable must be able to account for influences of neighboring ζ 's for near zero Peclet numbers and also eliminate influences of downwind ζ 's for $|P| \gg 0$.

The Hybrid scheme developed by Spalding [17] is a piecewise linear functional variation of ζ between two consecutive grid points. The term piecewise is used because one of three linear functions are chosen to represent the variation of ζ depending upon the value of the local Peclet number. Because the proper linear function is chosen based on the value of the local Peclet number some logic must be implemented into the function.

In the Hybrid scheme the logic is introduced to the linear function via coupling coefficients. The coupling coefficients come about by substituting the following expressions for the terms on the left of Equation (2.11):

$$(J_e - m_e \zeta_p) = a_E (\zeta_p - \zeta_E) , \quad (2.14a)$$

$$(J_w - m_w \zeta_p) = a_W (\zeta_W - \zeta_p) , \quad (2.14b)$$

$$(J_n - m_n \zeta_p) = a_N (\zeta_p - \zeta_N) , \quad (2.14c)$$

$$(J_s - m_s \zeta_p) = a_S (\zeta_S - \zeta_p) , \quad (2.14d)$$

where a_E , a_W , a_N , and a_S are the coupling coefficients for ζ_p and ζ_E , ζ_p and ζ_W , ζ_p and ζ_N , and ζ_p and ζ_S respectively. The coupling coefficients may be represented by the following logic functions:

$$a_E = \frac{\Gamma_{\zeta_e}}{\Delta x_e} r_p \Delta r [L0(0, 1-0.5|P_e|)] + L0(-m_e, 0) , \quad (2.15a)$$

$$a_W = \frac{\Gamma_{\zeta_w}}{\Delta x_w} r_p \Delta r [L0(0, 1-0.5|P_w|)] + L0(m_w, 0) , \quad (2.15b)$$

$$a_N = \frac{\Gamma_{\zeta_n}}{\Delta x_n} r_n \Delta x [L0(0, 1-0.5|P_n|)] + L0(-m_n, 0) \quad , \quad (2.15c)$$

$$a_S = \frac{\Gamma_{\zeta_s}}{\Delta x_s} r_s \Delta x [L0(0, 1-0.5|P_s|)] + L0(m_s, 0) \quad . \quad (2.15d)$$

The logic statement $L0(A,B)$ refers to the Larger Of the two terms (A,B). For example $L0(7, 5) = 7$ or $L0(-32.75, 1.598) = 1.598$.

As a verification that Equations (2.12) and (2.14a) are equivalent, Equation (2.12) will be expanded using central differencing and compared to Equation (2.14a) with $P_e \rightarrow 0$ (central differencing). Repeating Equation (2.12) here for convenience.

$$(J_e - m_e \zeta_p) = r_p \Delta r [(\rho u \zeta)_e - (\Gamma_{\zeta} \frac{\partial \zeta}{\partial x})_e] - (\rho u)_e r_p \Delta r \zeta_p \quad (2.12)$$

For the convection term $(\rho u \zeta)_e$ the natural choice for ζ_e would be

$$\zeta_e = \frac{1}{2} (\zeta_E + \zeta_p) \quad . \quad (2.16)$$

The factor 1/2 arises from the assumption of the interfaces being midway; some other factor would have appeared for differently located interfaces. The differential $(\partial \zeta / \partial x)_e$ may be written in a central difference form as

$$(\partial \zeta / \partial x)_e = (\zeta_E - \zeta_p) / \Delta x_e \quad . \quad (2.17)$$

Upon combining (2.16) and (2.17) with (2.12) the following discretized form of $(J_e - m_e \zeta_p)$ results:

$$(J_e - m_e \zeta_p) = r_p \Delta r \left[\frac{\Gamma_{\zeta_e}}{\Delta x_e} - \frac{1}{2} (\rho u)_e \right] (\zeta_p - \zeta_E) \quad . \quad (2.18)$$

When Equation (2.18) is compared to Equation (2.14a) the coupling coefficient a_E becomes

$$a_E = r_p \Delta r \left[\frac{\Gamma \zeta_e}{\Delta x_e} - \frac{1}{2} (\rho u)_e \right]. \quad (2.19)$$

A similar central difference analysis may be carried out for $(J_W - m_W \zeta_p)$ to give the following relations:

$$(J_W - m_W \zeta_p) = r_p \Delta r \left[\frac{\Gamma \zeta_W}{\Delta x_W} + \frac{1}{2} (\rho u)_W \right] (\zeta_W - \zeta_p), \quad (2.20)$$

and the coupling coefficient a_W may be written as

$$a_W = r_p \Delta r \left[\frac{\Gamma \zeta_W}{\Delta x_W} + \frac{1}{2} (\rho u)_W \right]. \quad (2.21)$$

As mentioned previously the central differencing scheme is equivalent to a local Peclet number near zero. Upon substitution of the near zero local Peclet numbers ($|P| < 2$) into Equations (2.15) and (2.16) respectively the following coupling coefficients are obtained

$$\begin{aligned} a_E &= \frac{\Gamma \zeta_e}{\Delta x_e} r_p \Delta r \text{LO} \left[0, 1 - \frac{1}{2} \frac{(\rho u)_e \Delta x_e}{\Gamma \zeta_e} \right] + \text{LO} [- (\rho u)_e \Delta r, 0] \\ &= r_p \Delta r \left[\frac{\Gamma \zeta_e}{\Delta x_e} - \frac{1}{2} (\rho u)_e \right], \quad \text{for } \left| \frac{(\rho u)_e \Delta x_e}{\Gamma \zeta_e} \right| \leq 2, \quad (2.22a) \end{aligned}$$

and

$$\begin{aligned} a_W &= \frac{\Gamma \zeta_e}{\Delta x_e} r_p \Delta r \text{LO} \left[0, 1 - \frac{1}{2} \left| \frac{(\rho u)_W \Delta x_W}{\Gamma \zeta_e} \right| \right] + \text{LO} [- (\rho u)_e \Delta r, 0] \\ &= r_p \Delta r \left[\frac{\Gamma \zeta_W}{\Delta x_W} + \frac{1}{2} (\rho u)_W \right], \quad \text{for } \left| \frac{(\rho u)_W \Delta x_W}{\Gamma \zeta_W} \right| \leq 2. \quad (2.22b) \end{aligned}$$

Equations (2.12) and 2.14a) may also be shown to be equivalent for $|P| > 2$ (upwind differencing). Also, similar expressions for the coupling coefficients a_N and a_S may be shown to follow the same rules as a_E and a_W adhere to respectively. Knowing this, the final form of the discretization equation may be written.

The final discretized equation is obtained by substitution of the appropriate terms into Equation (2.11). Upon substitution Equation (2.11) becomes

$$\begin{aligned} a_E(\zeta_P - \zeta_E) - a_W(\zeta_W - \zeta_P) + a_N(\zeta_P - \zeta_N) \\ - a_S(\zeta_S - \zeta_P) = (S_C - S_P \zeta_P) r_P \Delta x \Delta r \quad , \end{aligned} \quad (2.23a)$$

or rearranging terms, an equivalent expression results

$$a_P \zeta_P = a_E \zeta_E + a_W \zeta_W + a_N \zeta_N + a_S \zeta_S + \beta \quad (2.23b)$$

where

$$a_P = a_E + a_W - a_N + a_S - S_P (r_P \Delta x \Delta r) \quad , \quad (2.24a)$$

$$\beta = S_C (r_P \Delta x \Delta r) \quad . \quad (2.24b)$$

By now it can be appreciated that the physical significance of the various coupling coefficients in Equation (2.23b) is easy to understand. The neighboring coefficients a_E , a_W , a_N , and a_S represent the convection and diffusion influence at the four faces of the control volume.

2.3 Grid Systems and Dependent Variable Locations

Before the boundary conditions may be imposed on the discretized equations, a grid system or systems must be imposed upon the domain of interest. Three independent grid systems were chosen to represent the locations of various dependent variables. The three grid systems are displaced or "staggered". The "staggered" grid was first employed by Harlow and Welch [18] in their MAC method to overcome instabilities due to the placement of all the dependent variables on one grid system.

The grid systems used must conform to the two-dimensional axisymmetric differential equation presented in Section 2.1 of this Chapter. A 2-D axisymmetric non-uniform grid system may be represented by the planar system shown in Figure 2. Figure 2 is a cut-away view of the 2-D axisymmetric grid system. A perspective view of the P-CELL is shown in Figure 3 which exemplifies the 2-D axisymmetric property of angular independence. The grid system presented in Figure 2 will be referred to as the "main" grid system, where the dependent variables P and T are evaluated at the intersection of the grid lines.

The displaced grid systems, referred to as the u- and v-grid system, are represented by the dashed lines in Figures 4 and 5, respectively. The main grid is also presented in Figures 4 and 5; it is represented by the solid lines. The u- and v- cells are associated with the grid point P. The dependent variables u and v are evaluated at the intersection of the dashed and solid lines in their respective grid system.

With the general discretized equation established, the grid systems defined, and the evaluation points of the dependent variables located, the specific discretized equations may now be presented.

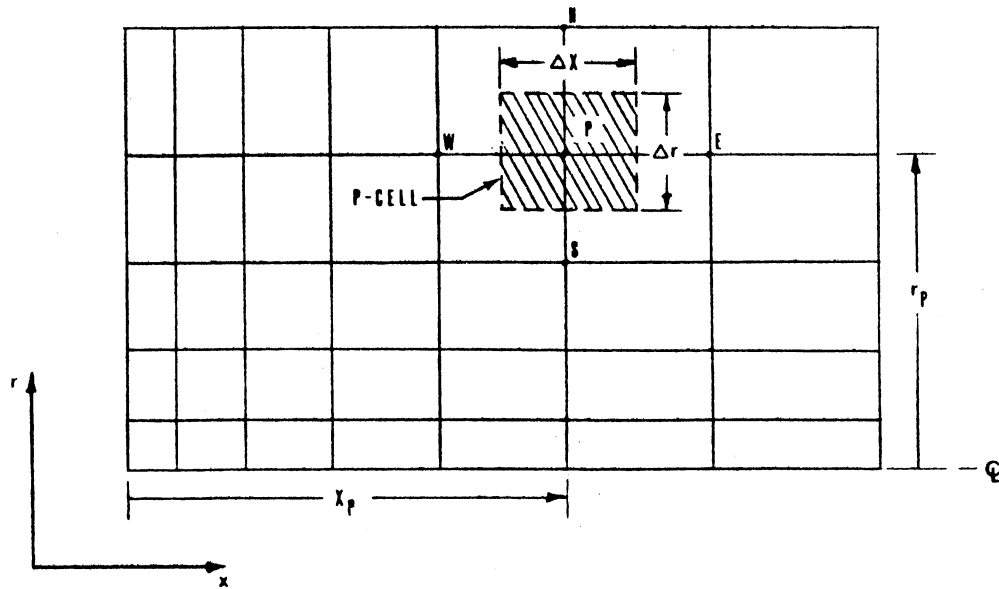


Figure 2. Two-Dimensional Axisymmetric Grid System

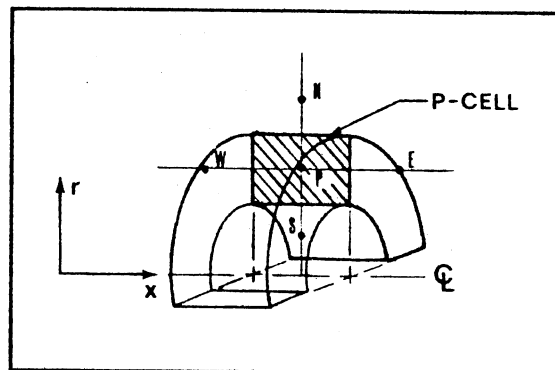


Figure 3. Perspective View of P-CELL

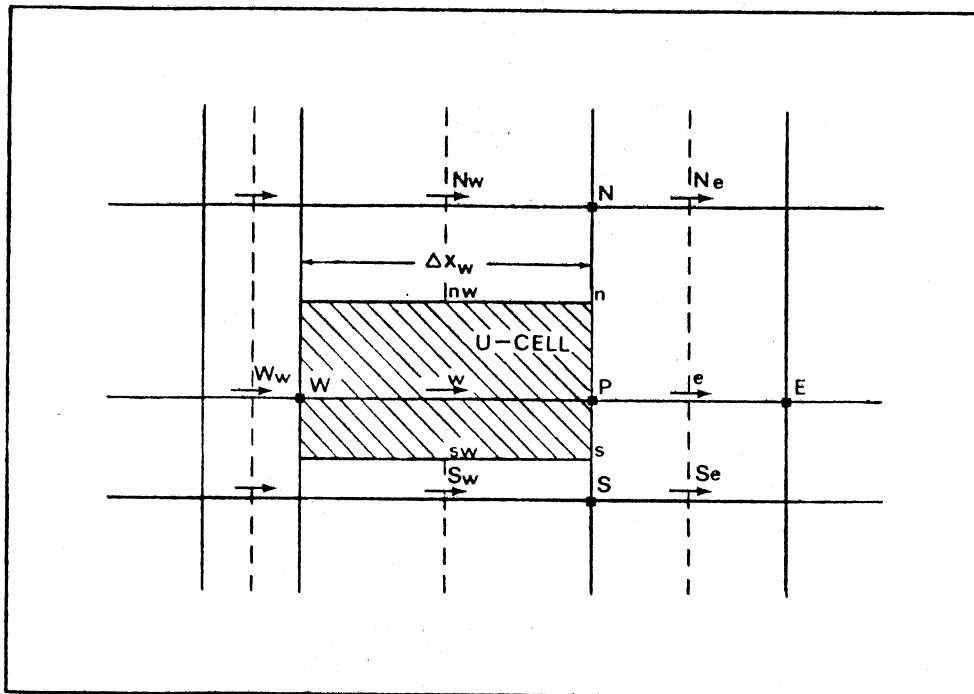


Figure 4. u-Grid System

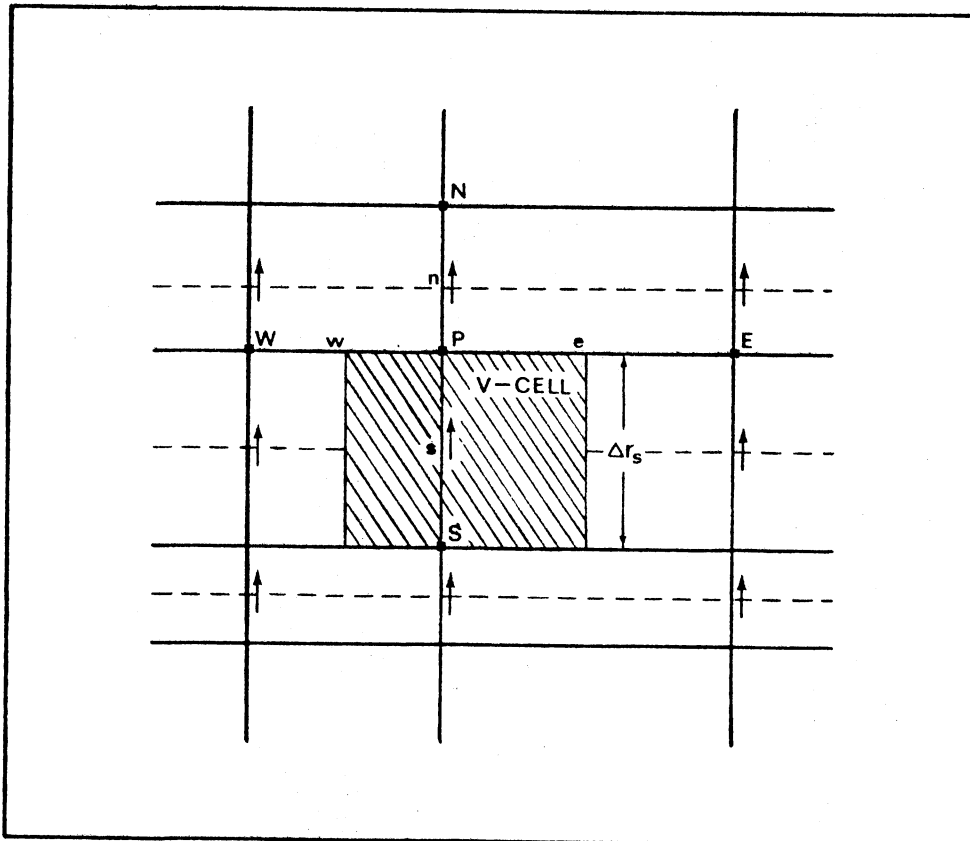


Figure 5. v-Grid System

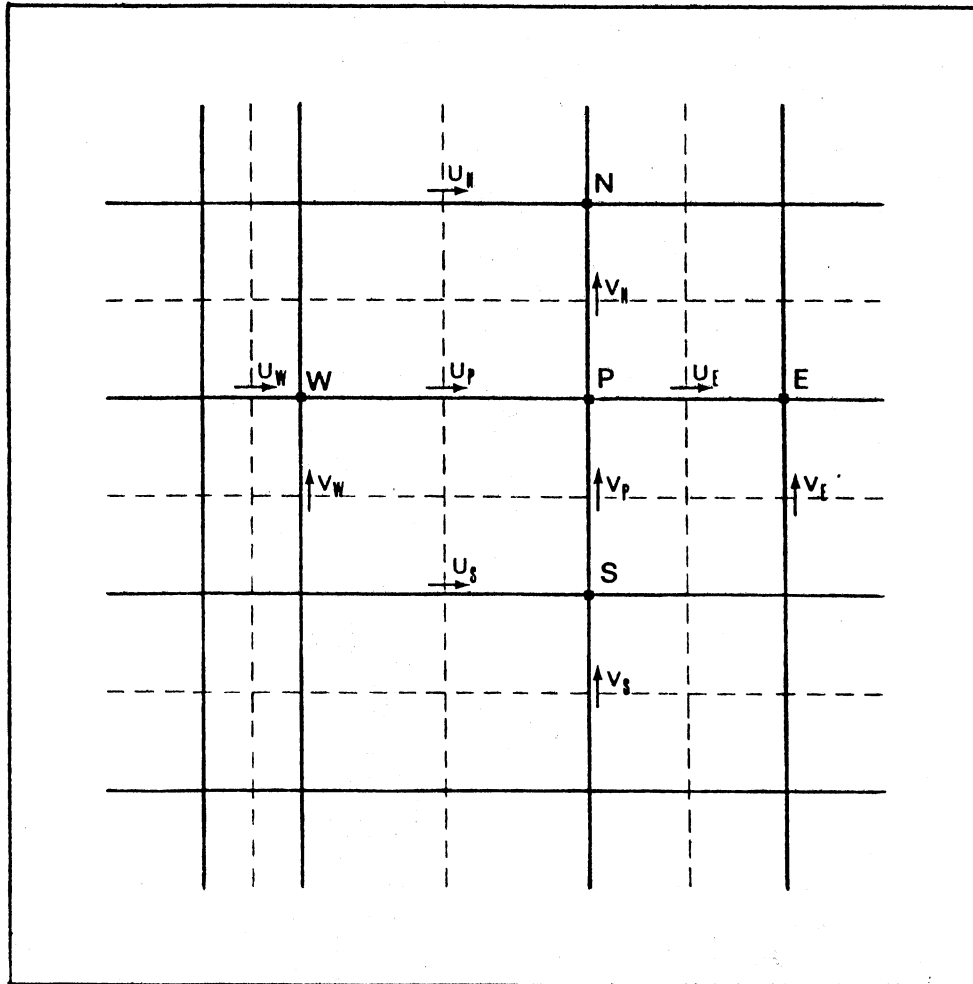


Figure 6. u- and v-Velocity Subscript Definition

2.4 Specific Discretized Equations

Since the u-CELL is associated with the point P the neighboring u-velocities will be defined as in Figure 6. The v-velocities are defined in a similar fashion. The specific discretized equations may now be written as follows:

u-Momentum

$$a_{p_u} u_p = a_{E_u} u_E + a_{W_u} u_W + a_{N_u} u_N + a_{S_u} u_S - r_p \Delta r (P_W - P_P) + \beta \quad (2.25)$$

where

$$a_p = a_{E_u} + a_{W_u} + a_{N_u} + a_{S_u} \quad (2.25a)$$

$$\left(S_p + \frac{\mu_W}{r_p} \right) (r_p \Delta x_W \Delta r) \quad ,$$

$$\beta = S_c (r_p \Delta x_W \Delta r) \quad (2.25b)$$

The coupling coefficients are determined from Equations (2.15a), (2.15b), (2.15c), and (2.15d) with appropriate μ 's chosen for Γ_ζ 's and proper distances substituted for the Δ 's.

v-Momentum

$$a_{p_v} v_p = a_{E_v} v_E + a_{W_v} v_W + a_{N_v} v_N + a_{S_v} v_S + r_s \Delta x (P_S - P_P) + \beta \quad (2.26)$$

where

$$a_{p_v} = a_{E_v} + a_{W_v} + a_{N_v} + a_{S_v} \quad -$$

$$\left(S_p + \frac{\mu_S}{r_s} \right) (r_s - \Delta x \Delta r_s) \quad , \quad (2.26a)$$

$$\beta = S_c (r_s - \Delta x \Delta r_s) . \quad (2.26b)$$

are determined in a similar manner as the u-Momentum. Note that the pressure gradient term $r_s \Delta x (P_s - P_p)$ has been pulled out of the source terms in both momentum equations. Because the pressure field is ultimately calculated, it would be inconvenient to bury the pressures in the momentum source terms.

Energy

$$a_p T_p = a_E T_E + a_W T_W + a_N T_N + a_S T_S + \beta , \quad (2.27)$$

where

$$a_p = a_E + a_W + a_N + a_S - S_p r_p \Delta x \Delta r , \quad (2.27a)$$

$$\beta = S_c r_p \Delta x \Delta r . \quad (2.27b)$$

The coupling coefficients are found by substituting μ/Pr or k/C_p for Γ_{ζ_e} in Equations (2.15a-d).

The pressure-update equation is obtained through the continuity equation. Since the velocity and pressure fields are unknown boundary conditions and an initial guess of the field variables are necessary. The guessed pressure field denoted by P^g , must be updated or improved so that the resulting guessed velocity fields u^g and v^g satisfy the continuity equation at all grid locations. Once the guessed field variables have been updated the updated field variables are then used as a modified guess of the field variables (i.e., after updating u , $u^g = u$).

The velocity-update equations may be written as

Velocity-Update Equation

$$u_p = u_p^g + r_p \Delta r (P_W^c - P_p^c) , \quad (2.28a)$$

$$v_p = v_p^g + r_s \Delta x (P_S^c - P_p^c) , \quad (2.28b)$$

where the superscript c refers to correction terms. If $P = P^g + P^c$, then as the correction term P^c approaches zero P^g approaches the correct pressure field P . The same may be said about Equations (2.28a) and (2.28b); as P^c approaches zero u_p^g and v_p^g approach the correct velocity fields u_p and v_p respectively. The correct velocity fields must satisfy the continuity.

To insure that the velocity fields satisfy the Continuity Equation the pressure correction P^c must also conform to the Continuity Equation. This may be done by integrating the Continuity Equation about the P-CELL and substituting the appropriate velocity correction formulas (2.28a) or (2.28b) for the velocity components obtained from the P-CELL integration. The resulting discretized Pressure-Update Equation is given as

Pressure-Update Equation

$$a_p P_p^c = a_E P_E^c + a_W P_W^c + a_N P_N^c + a_S P_S^c + \beta , \quad (2.29)$$

where

$$a_E = \rho_e (r_p \Delta r^2) / a_{p_u} , \quad (2.29a)$$

$$a_W = \rho_w (r_p \Delta r^2) / a_{p_u} , \quad (2.29b)$$

$$a_N = \rho_n (r_n \Delta x^2) / a_{p_v} , \quad (2.29c)$$

$$a_{\chi} = \rho_S (r_S \Delta x^2) / a_{P_V} , \quad (2.29d)$$

$$a_P = a_E + a_W + a_N + a_S , \quad (2.29e)$$

$$\beta = [m_W^g - m_e^g] + [m_S^g - m_n^g] \quad (2.29f)$$

The guessed mass flow, into the eastern face of the P-CELL is given by

$$m_e^g = \rho_e u_p^g r_p \Delta r . \quad (2.30)$$

β in Equation (2.29f) is the total mass flux through the P-CELL. As successive updates are made on the velocity fields β will tend to zero. For $\beta = 0$ the Continuity Equation is exactly satisfied and no pressure correction is needed. This would indicate the solution for the flow field is complete. The sequence of operations required to determine the field variables is illustrated in the flow chart in Appendix A.

The implementation of the boundary conditions to the discretized equations is the only concept lacking in determining the field solution to the governing differential equations. This will be discussed in the upcoming Section 2.5.

2.5 Implementation of Boundary Conditions

The control-volume method is extremely useful when considering boundary conditions. This method will be employed here to derive the discretized boundary conditions.

Figure 7 shows how a northern boundary would be placed midway between two consecutive horizontal gridlines. Southern, eastern, and western boundaries are handled in a similar fashion. The location of the P, u, and v-CELLS are also presented in Figure 7.

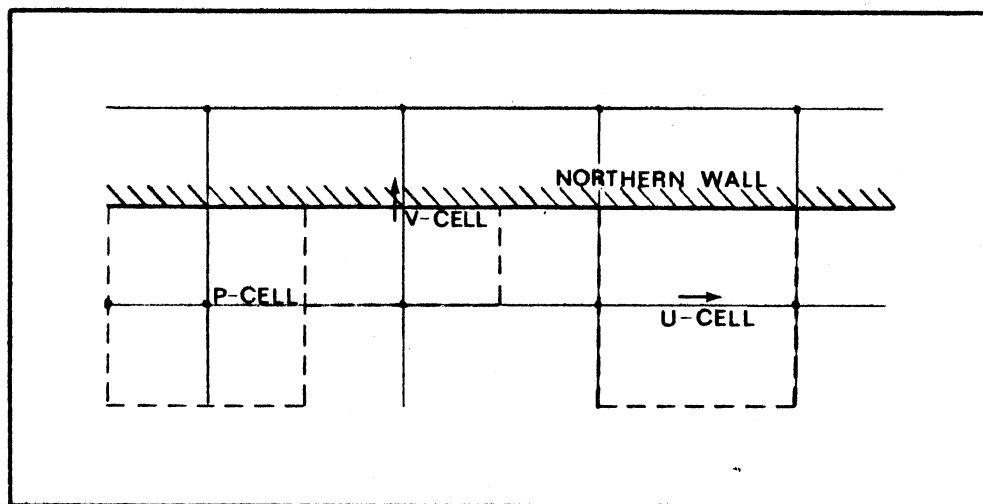


Figure 7. Northern Boundary

There are essentially two types of boundary conditions. The first is the impervious boundary where convection is zero; this may be a wall where no flow is allowed to cross. The second is an inlet or outlet boundary where fluid is allowed to enter or exit the domain of interest across the boundary.

It must be noted that for a specification of a known normal velocity on a boundary it is not necessary to specify the boundary pressure. Conversely if a boundary pressure is specified the normal velocity need not be specified. This stems from the fact that for a known normal wall velocity $v = v^g$ the correcting pressure gradient of Equation (2.28a) or (2.28b) is not used. Thus, $(p_P^g - p_N^g)$ will not appear, or a_N will be zero in the Pressure-Update Equation (2.29). This means that no information is needed about p_N^g .

To correctly specify boundary conditions the discretized equation must be modified for the near boundary points. The northern boundary and near boundary P-CELL will be used to construct the general modified discretized boundary equations as depicted in Figure 8.

For an impervious or non-convective boundary the influence of the northern dependent variable ζ_N must be eliminated and a new influence inserted via the source terms. The convective influence of ζ_N may be eliminated by setting the total ζ_{flux} through the northern boundary a_N to zero. Because this also eliminates the diffusive flux term $\Gamma_\zeta \frac{\partial \zeta}{\partial r}$ it must be transferred to the right hand side of Equation (2.23). Equation (2.23b) is repeated here for convenience.

$$[a_E + a_W + a_N + a_S - S_p (r_p \Delta r \Delta x)] \zeta_p =$$

$$a_E \zeta_E + a_W \zeta_W + a_N \zeta_N + a_S \zeta_S + S_c (r_p \Delta r \Delta x) . \quad (2.23b)$$

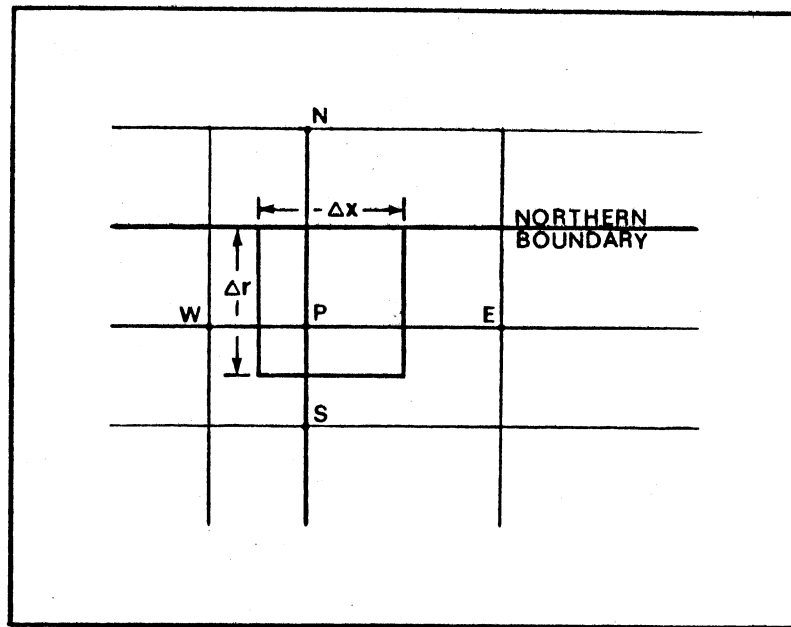


Figure 8. Northern Boundary with Near Boundary P-CELL

If the diffusion term is known on the northern boundary then

$$a_N = 0 \quad , \quad (2.31)$$

$$S_c (r_p \Delta r \Delta x) = \left(\Gamma_\zeta \frac{\partial \zeta}{\partial r} \right)_{\text{wall}} \quad , \quad (2.32)$$

$$S_p = 0 \quad . \quad (2.33)$$

Equation (2.23b) becomes

$$(a_E + a_W + a_S) \zeta_p = a_E \zeta_E + a_W \zeta_W + a_S \zeta_S + \left(\Gamma_\zeta \frac{\partial \zeta}{\partial r} \right)_{\text{wall}} \quad . \quad (2.34)$$

This type of boundary condition could represent a given heat flux on the outer wall of a duct where $\Gamma_\zeta \frac{\partial \zeta}{\partial r} = \Gamma_\zeta \frac{\partial T}{\partial r} = - \dot{q}_W'' / C_p$ in Equation (2.32).

For an impervious boundary where ζ is specified ζ_N must again be eliminated by setting the coupling coefficient a_N to zero. The influence of the wall ζ is incorporated into the discretized equation by creating a representative coupling coefficient given by

$$a_{\text{wall}} = \Gamma_\zeta \frac{\Delta x r_{\text{wall}}}{\left(\frac{1}{2} \Delta r \right)} \quad , \quad (2.35)$$

and inserting a_{wall} into the linearized source term. The coefficients of the linearized source term become

$$S_c (r_p \Delta r \Delta x) = a_{\text{wall}} \zeta_{\text{wall}} \quad , \quad (2.36a)$$

$$S_p (r_p \Delta r \Delta x) = -a_{\text{wall}} \quad . \quad (2.36b)$$

The resulting discretized equation is given as:

$$\begin{aligned} & [a_E + a_W + a_S + a_{\text{wall}}] \zeta_p = \\ & a_E \zeta_E + a_W \zeta_W + a_S \zeta_S + a_{\text{wall}} \zeta_{\text{wall}} \quad . \end{aligned} \quad (2.37)$$

In effect an approximation to the wall gradient $\partial\zeta/\partial r$ has been made. This can be seen by transferring the $a_{\text{wall}} \zeta_p$ term to the right hand side of Equation (2.37) forming the term $a_{\text{wall}}(\zeta_{\text{wall}} - \zeta_p)$ which may be expanded to give

$$a_{\text{wall}}(\zeta_{\text{wall}} - \zeta_p) = \Gamma_{\zeta} (r_{\text{wall}} \Delta x) (\zeta_{\text{wall}} - \zeta_p) / \left(\frac{1}{2} \Delta r\right) \quad (2.38)$$

where $(\zeta_{\text{wall}} - \zeta_p) / (1/2 \Delta r)$ is nothing more than an approximation of the wall gradient $\partial\zeta/\partial r$. Boundary conditions of this type would be used for specifying T, u, v, or P on impervious boundaries.

The non-impervious boundaries, those that may occur at an inlet or outlet, are treated by knowing either the boundary value ζ_b or the gradient at the boundary. For an impervious boundary where ζ_b is known no modifications to the discretized equations are needed. Since ζ_b lies on the boundary and convection occurs across the boundary, no modification to the coupling coefficients are necessary. Consequently, no modifications to the linearized source terms are necessary.

A non-impervious boundary where the normal gradient is known at the boundary is handled in exactly the same manner as the impervious wall with the boundary diffusion term specified, only the coupling coefficient is not set to zero. This allows the proper convection to take place across the boundary.

A special boundary condition which might be used to specify a moving boundary or blockage in the flow field would be the specification of a grid point to a value ζ_F . For this type of boundary condition ζ_F must be dominant in the general discretized equation. The domination of ζ_F is accomplished in the following manner:

Set

$$S_c (r_p \Delta r \Delta x) = \zeta_F (1 \times 10^{30}) , \quad (2.39a)$$

$$S_p (r_p \Delta r \Delta x) = - (1 \times 10^{30}) , \quad (2.39b)$$

giving rise to the discretized equation

$$\begin{aligned} & [a_E + a_W + a_N + a_S] \zeta_p + (1 \times 10^{30}) \zeta_p = \\ & [a_E \zeta_E + a_W \zeta_W + a_N \zeta_N + a_S \zeta_S] + (1 \times 10^{30}) \zeta_F . \end{aligned} \quad (2.40)$$

It can be seen that $(1 \times 10^{30}) \zeta_p$ and $(1 \times 10^{30}) \zeta_F$ are the dominating terms of the discretized Equation (2.40) giving rise to the solution $\zeta_p = \zeta_F$.

A final note concerning boundary conditions for the u- and v-grid systems must be conveyed. Because the u- and v-grid systems are shifted from the main grid it will be necessary to re-evaluate the linearized source terms in such a way that the discretized boundary equations reflect the integration of the governing differential equations over a partial cell.

2.6 Summary

In this Chapter the governing differential equations for two-dimensional axisymmetric laminar flow were all reduced to one common differential equation. This general differential equation was integrated over a control volume (a subdomain of the region of interest) utilizing piecewise functional variations of the dependent variable, ζ , between grid points. This integrand and the Continuity Equation were amalgamated to form the general discretized Equation

(2.23b). The main-, u-, and v-grid systems were also presented, so that the specific discretized equations for u , v , T , and P could be formulated.

The discretized equations and grid systems of Sections 2.1 - 2.4 were presented as background material for the implementation of boundary conditions presented in Section 2.5. The boundary conditions for various convective and non-convective boundaries were derived and the domination of fixed value boundaries were introduced into the general discretized equation.

CHAPTER III

VARIABLE-PROPERTY METHOD

For internal convective flow heat transfer problems, where velocity and temperature profiles are simultaneously developing and the wall to inlet temperature ratios deviate from unity a variable-property technique should be employed to insure that a realistic solution is obtained. There are essentially two ways to correct temperature-dependent property solutions. One method is to solve for the constant property solution and use a reference temperature or property ratio scheme to correct for property variations. The other method is to use physical-property equations to update properties as a numerical solution converges. These two methods for solving the temperature-dependent-property solution will be discussed. Also, the reasons for choosing the thermo-physical-property update method when solving thermo-fluid problems by finite difference techniques will be made clear.

3.1 Reference Temperature and Property Ratio Methods

The reference temperature method utilizes a characteristic temperature where properties appearing in the non-dimensional groups (Re , Nu , Pr , etc.) may be evaluated so that the constant-property results at the characteristic temperature may be used in determining the variable-property behavior. Typically this reference temperature is the wall temperature or mixed mean temperature; there is no general rule.

The property ratio method involves using viscosity ratios for liquids where viscosity variations are responsible for most of the variable-property effects and absolute temperature ratios for gases where viscosity, thermal conductivity, and density changes are responsible for the variable-property effects. For gases the absolute temperature dependence is similar for different gases; although, this similarity no longer holds true at extreme temperatures. The relation used to correct the constant-property model, (CP), for gases is given as

$$\frac{Nu}{Nu_{CP}} = \frac{St}{St_{CP}} = \left(\frac{T_w}{T_m} \right)^n \quad (3.1)$$

$$\frac{C_f}{C_{f_{CP}}} = \left(\frac{T_w}{T_m} \right)^m \quad (3.2)$$

where the subscripts w and m refer to the wall and mixed mean temperatures, respectively.

All properties in the non-dimensional groups are evaluated at mixed mean temperatures. The exponents m and n are functions of geometry and types of flow which are determined experimentally. Thus, for a given heating and flow situation m and n may be selected and used in Equations (3.1) and (3.2) to determine the variable-property solution.

It is important to note that the reference temperature and property ratio methods have been applied to only a fraction of the geometries and boundary conditions for which constant property solutions are available. This is because the results must be correlated for a specific tube cross section, tube wall boundary condition, and flow orientation [19].

3.2 Thermo-Physical-Property Update Method

The thermo-physical-property update method uses physical-property equations for k , μ , C_p and the ideal gas law for ρ when dealing with gases at low pressures. When new update temperatures are determined after a complete sweep of the grid system, the thermo-physical equations are applied to each grid point so that new updates of the physical properties may be made. This enables the property and thermo-fluid solutions to converge simultaneously, resulting in a realistic solution to the governing two-dimensional axisymmetric Equations, (2.1) through (2.4) with temperature-dependent properties.

The physical-property equations used in the thermo-physical-property update method may be found for most common fluids in general engineering handbooks. For example, the physical-property equations for air are:

thermal conductivity [20]

$$k = 4186 (6.325 \times 10^{-7} (T^{1.5})) / (T + 245.4 \times 10^{-(12/T)}) \quad \text{W/(m-K)}, \quad (3.3)$$

viscosity [20]

$$\mu = (1.458 \times 10^{-6} (T^{1.5})) / (T + 110.4) \quad \text{Kg/(m-s}^2\text{)} , \quad (3.4)$$

specific heat [21]

$$C_p = 4184 (0.244388 - 4.20419 \times 10^{-5}T + 9.61128 \times 10^{-8}T^2 - 1.16383 \times 10^{-11}T^3) \quad \text{J/(Kg - K)} , \quad (3.5a)$$

for $250^0\text{K} < T \leq 600^0\text{K}$,

$$C_p = 4184 (0.208831 + 7.71027 \times 10^{-5}T - 8.56726 \times 10^{-9}T^2 - 4.75772 \times 10^{-12}T^3) \quad \text{J/(Kg - K)} \quad (3.5b)$$

for $600^{\circ}\text{K} < T < 1500^{\circ}\text{K}$,

density

$$\rho = P/(287 \cdot T) \quad \text{Kg/m}^3, \quad (3.6)$$

where T is the absolute temperature in degrees Kelvin and Pressure, P , is specified in Pascals.

It is important to note that the physical-property equations are not limited by tube geometry, boundary conditions, or flow orientation. The only limitation on the physical-property equations is their accuracy in reproducing experimental results. The equations were compared to tabulated data of Kays and Crawford [21]. The mean and maximum percent deviation are given in Table II for the temperature range $100^{\circ}\text{K} \leq T \leq 1000^{\circ}\text{K}$.

3.3 Summary

Three variable-property techniques used in determining a solution for thermo-fluid property-varying problems have been presented. The reference temperature and property ratio methods utilize the constant-property solution to correct for property variations. The reference temperature method is awkward to use for internal flow problems and the property ratio method is limited to known n and m exponents reported for specific tube geometries, boundary conditions, and flow orientations. However, the thermo-physical-property update method is only limited by the accuracy of the physical-property equations.

TABLE II

MEAN AND MAXIMUM PERCENT DEVIATIONS FOR PROPERTY-EQUATION
OF AIR EVALUATED AT STANDARD ATMOSPHERIC PRESSURE

Property Equation	Mean Deviation (%)	Maximum Deviation (%)
Thermal Conductivity	0.934	2.32
Viscosity	0.481	0.60
Specific Heat	0.060	0.295
Density	0.049	0.212

The thermo-physical-property updated method is introduced in the TEACH code when solving the thermo-fluid property-varying problem for channel flow. This will be presented in Section 4.2 as a study of how property-variations influence heat transfer in the entrance region between two semi-infinite parallel plates.

CHAPTER IV

NUMERICAL STUDY OF LAMINAR FORCED CONVECTION HEAT TRANSFER IN THE ENTRANCE REGION OF A FLAT DUCT

The analysis of forced convective heat transfer in the entrance region of various two-dimensional axisymmetric geometries has been analyzed by many different techniques. These forced convective heat transfer problems do not easily lend themselves to an exact analytical solution because of their complex governing differential equations. The material presented in Chapter IV is primarily concerned with laminar forced convection heat transfer in the entrance region of a flat duct with uniform wall temperature.

Sparrow [13] first investigated heat transfer between parallel plates using the Karman-Pohlhausen method to determine a solution for uniform wall temperature on both plates. Hawang and Fan [14] used the finite difference analysis developed by Bodoia and Osterle [23] to solve the two-dimensional continuity and momentum equations with the usual Prandtl boundary layer assumptions. The velocity profiles are then used to solve the two-dimensional energy equation with the absence of axial heat conduction. The results of Hawang and Fan [14] are in close agreement with those of Sparrow [13] for Pr greater than 0.1. An approximate analytical procedure developed by Bhatti and Savery [24] uses mechanical energy equations to determine an axial core velocity which is in turn used to solve for temperature profiles by the Karman-

Pohlhausen method. Their results predict lower local Nusselt numbers than those obtained by Hawang and Fan [14].

Mercer et al. [3] developed an analytical model for the simultaneously developing region between parallel plates and supplemented this work by performing an experimental analysis for air. Mercer et al. compared their analytical and experimental results and reported a 5 percent deviation between the two. Recently, Narang and Hussain [3] used an analytical solution of the linearized momentum equations developed by Narang and Krishnamoorthy [25] to solve the exact energy equation by a successive over-relaxation method. Their results will be compared to the constant property model of the present work in Section 4.1.

The above mentioned analytical methods [3, 4, 13, 14, 23, 24, and 25] either assume the transverse momentum to be negligible compared to the axial momentum or the momentum equations have been linearized by assuming that the inertia forces are most significant in the entry region. Also, in all the aforementioned models for the combined entry region the energy and momentum equations have been decoupled by assuming that the thermophysical properties of the fluid are constant. This allows the temperature solution to be solved once the velocity solution has been determined.

In the present analysis the energy and momentum equations are first decoupled by assuming constant properties but no generality of the conservation equations are lost. Section 4.1 discusses the results of the constant-property model and compares the results with other analytical results. Section 4.2 discusses the results of the coupled variable-property model and comparisons are made with the experimental

work of Mercer, Pearce and Hitchcock [4]. The effects of varying properties on non-dimensional heat transfer coefficients will be referred to in Section 4.3.

4.1 Results of Constant-Property Model

The two-dimensional laminar flow between two semi-infinite parallel plates is shown in Figure 9. The fluid properties are assumed to remain constant throughout and the flow experiences no viscous dissipation. The governing differential equations which describe these conditions are:

Continuity

$$\frac{\partial}{\partial x} (\rho u) + \frac{\partial}{\partial r} (\rho v) = 0 \quad (4.1)$$

u-Momentum

$$\frac{\partial}{\partial x} (u \rho u) + \frac{\partial}{\partial r} (v \rho u) = - \frac{\partial P}{\partial x} + \frac{\partial}{\partial x} \left(\mu \frac{\partial u}{\partial x} \right) + \frac{\partial}{\partial r} \left(\mu \frac{\partial u}{\partial r} \right) \quad (4.2)$$

v-Momentum

$$\frac{\partial}{\partial x} (u \rho v) + \frac{\partial}{\partial r} (v \rho v) = - \frac{\partial P}{\partial r} + \frac{\partial}{\partial x} \left(\mu \frac{\partial v}{\partial x} \right) + \frac{\partial}{\partial r} \left(\mu \frac{\partial v}{\partial r} \right) \quad (4.3)$$

Energy

$$\frac{\partial}{\partial x} (\rho u T) + \frac{\partial}{\partial r} (\rho v T) = \frac{\partial}{\partial x} \left(\frac{k}{C_p} \frac{\partial T}{\partial x} \right) - \frac{\partial}{\partial r} \left(\frac{k}{C_p} \frac{\partial T}{\partial r} \right) \quad (4.4)$$

where the properties are left within the derivatives so as not to lose any generality when the variable-property model is discussed in Section 4.2. The variable r is used here to describe the vertical distance rather than the conventional notation y ; this is so that notational consistency is maintained throughout this report.

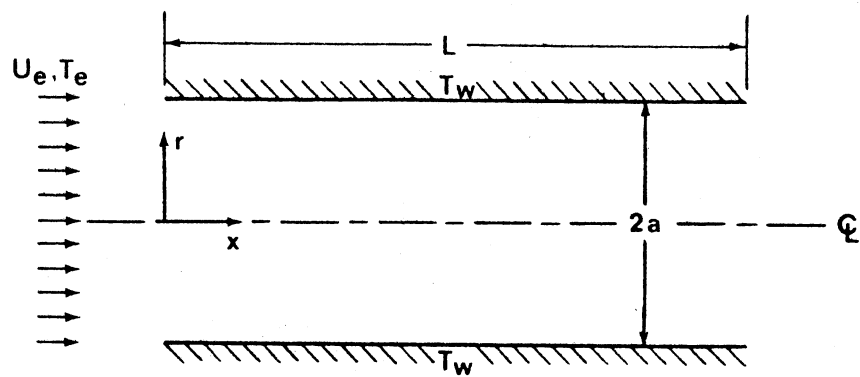


Figure 9. Geometry of Problem

The boundary conditions which describe the limits of the domain depicted in Figure 9 are:

$$u(0,r) = U_e \quad (4.5a)$$

$$\frac{\partial}{\partial x} (\rho u(L_\infty, r)) = 0 \quad (4.5b)$$

$$u(x, \pm a) = 0 \text{ or } u(x, a) = 0, \frac{\partial}{\partial r} (\rho u(x, 0)) = 0 \quad (4.5c)$$

$$v(0,r) = 0 \quad (4.6a)$$

$$v(L_\infty, r) = 0 \quad (4.6b)$$

$$v(x, \pm a) = 0 \text{ or } v(x, a) = 0, v(x, 0) = 0 \quad (4.6c)$$

$$T(0,r) = T_e \quad (4.7a)$$

$$\frac{\partial}{\partial x} (T(L_\infty, r)) = 0 \quad (4.7b)$$

$$T(x, \pm a) = T_w \text{ or } T(x, a) = T_w, \frac{\partial}{\partial r} (T(x, 0)) = 0 \quad (4.7c)$$

These boundary conditions were implemented in the TEACH code by the methods outlined in Section 2.4.

The temperature and velocity fields were determined and the local Nusselt numbers were calculated. The local Nusselt numbers Nu_x may be determined by equating the local heat flow at the channel's wall; that is

$$\dot{q}_w'' = h(T_w - T_m) = -k \left. \frac{\partial T}{\partial r} \right|_{r=a}, \quad (4.8)$$

where mixed mean fluid temperature, T_m is determined by

$$T_m = \frac{1}{A_c V} \int_{A_c} (uT) dA_c, \quad (4.9)$$

and the average velocity V is calculated as follows:

$$V = \frac{1}{A_c} \int_{A_c} (u) dA_c \cdot \quad (4.10)$$

Nu_x is found from Equation (4.8) to be

$$Nu_x = \frac{hd}{k} = \frac{-(4a)}{(T_w - T_m)} \left. \frac{\partial T}{\partial r} \right|_{r=a} \cdot \quad (4.11)$$

Before the final results for both the constant- and variable-property model were determined to be acceptable, the expanding grid system was refined to a 20 by 21 grid system. With this grid arrangement the results did not produce significant deviations with an increase in the number of gridpoints.

A comparison of the present results of the local Nusselt numbers with those determined by Narang and Hussain [3] for a Prandtl number of 0.7 and Reynolds numbers of 20 and 1000 may be found in graphical form in Figures 10 and 11 respectively. For the near slug flow analysis ($Re_d = 20$) the present results are within 5 percent of those of Narang and Hussain [3]. The local Nusselt numbers of the present results also compare well with [3] for $Re_d = 1000$ and $X > 0.02$, but significant deviations occur for the near inlet region ($X < 0.02$). This deviation is attributed to the linearization of the inertia terms in [3].

The constant-property results of the present work deviate only 2 percent from the values predicted by the numerical solution of Mercer, Pearce, and Hitchcock [4] for $Re_d = 682$ and $Pr = 0.7$. This case is presented in Section 4.2 where the constant- and variable-property models are compared to experimental results. The constant-property results of [4] would be overshadowed by the curve labeled CONSTANT-PROPERTY in Figure 12.

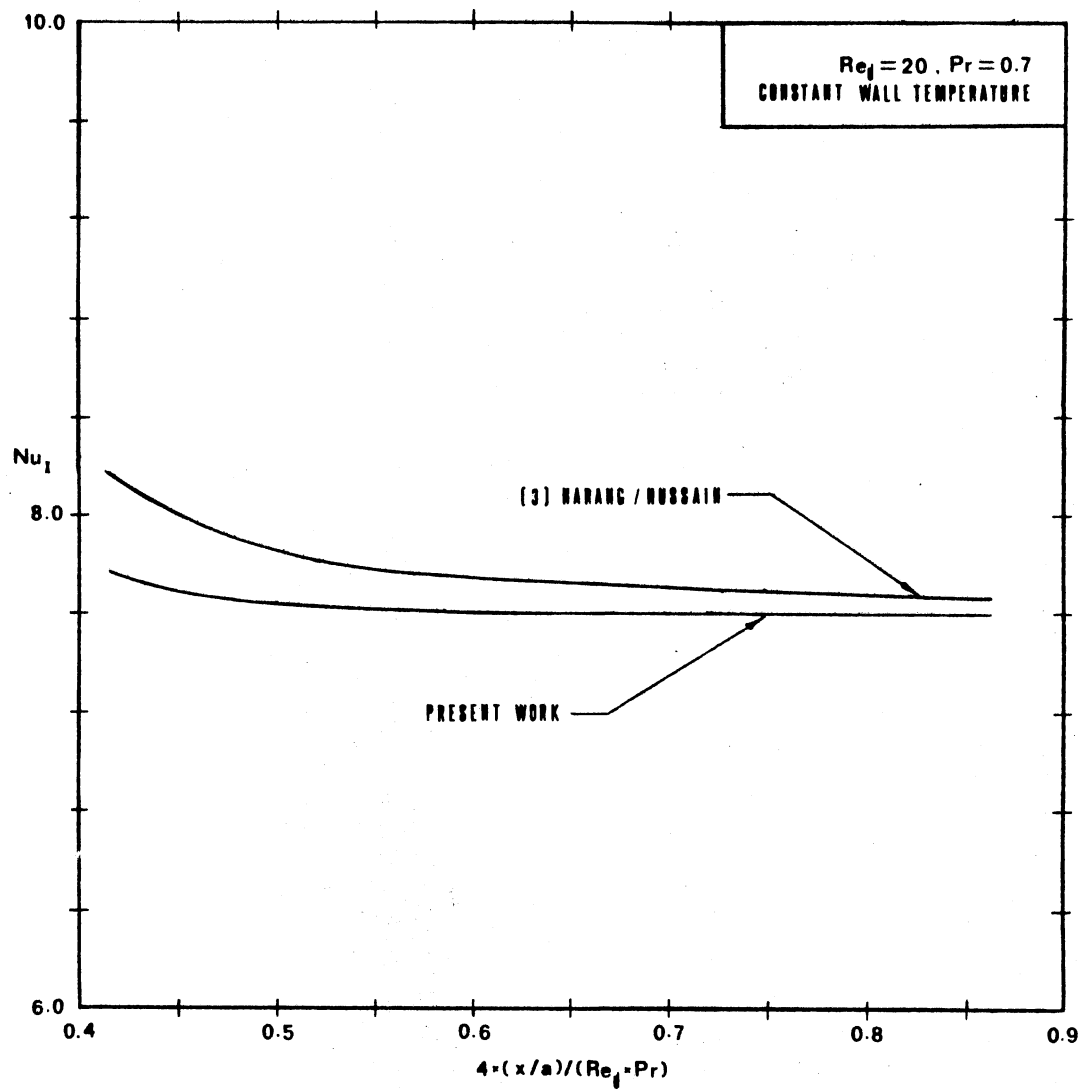


Figure 10. Comparison of Constant-Property Results with [3] for $Re_d = 20$

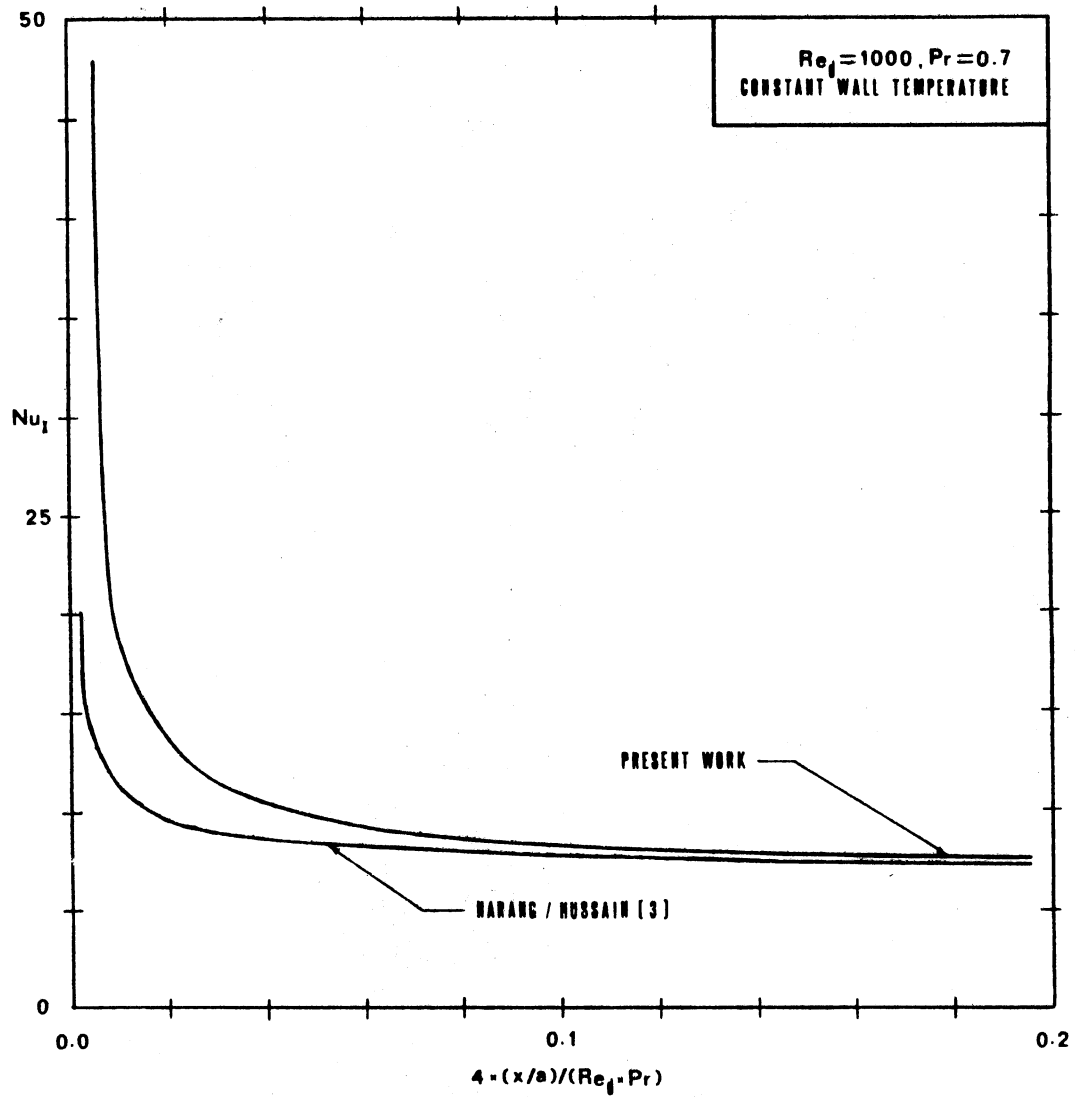


Figure 11. Comparison of Constant-Property Results with [3] at $Re_d = 1000$.

The present constant-property model also predicts the asymptotic local Nusselt value for constant wall temperature given by Kays and Crawford [22] as 7.54.

The results presented thus far indicate that the present constant-property model is in good agreement with the more recently proposed models [3, 4]. But, upon comparison of the constant-property model with experimental results for air of Mercer et al. [4] a uniform over prediction of Nu_x was noticed. Further investigations were performed and the variable-property method outlined in Section 3.2 was proposed to eradicate this discrepancy. The results from this investigation are presented in Section 4.2.

4.2 Results of the Variable-Property Model

The geometry, governing equations, and boundary conditions are the same as those given in Section 4.1. The variable-property method of Section 3.2 was incorporated into TEACH using the physical property equations for air. Because the properties of air vary according to the physical-property equations the Prandtl number will also vary. Thus, the Prandtl number at the entrance of the channel, Pr_e , will be used when referring to a particular variable-property case.

Temperature, velocity, pressure, and property fields were solved by under-relaxing the discretized equations of Section 2.2. The number of iterations to achieve a variable-property solution was found to be approximately 1.5 times that for the constant-property solution. The present results are compared with the experimentally determined Nusselt numbers of Mercer, Pearce, and Hitchcock [4] for air at an inlet Reynolds number of 682 and 1474.

The local Nusselt numbers based on the inlet fluid temperature T_e of [4] are calculated from the following relation:

$$Nu_{10} = \left(\frac{\partial \theta'}{\partial Y} \right) \text{ at } Y = 0, \text{ or } Y = 1, \quad (4.12)$$

where $\theta' = (T_w - T) / (T_w - T_e)$ and $Y = r/(2a)$. The local Nusselt number of the present work based on the mixed mean temperature, T_m , may be expressed in a similar form by

$$Nu_x = \left(\frac{\partial \theta}{\partial R} \right) \text{ at } R = 0, \text{ or } R = 1, \quad (4.13)$$

where $\theta = (T_w - T) / (T_w - T_m)$ and $R = r/(2a)$. Upon equating T_w in Equations (4.12) and (4.13) the following local Nusselt conversion relation is obtained:

$$Nu_{10} = \frac{1}{2} Nu_x \left(\frac{T_w - T_m}{T_w - T_e} \right). \quad (4.14)$$

The mixed mean temperatures of Mercer, et al. were not available. However, mixed mean temperatures of the present work were used to convert present Nu_x 's to equivalent Nu_{10} 's.

In the experimental analysis of [4] both uniform plate temperatures were reported to be 330.4⁰K and the inlet air temperature was reported to vary during the days of testing from 291.5 to 297.0⁰K. Substitution of the reported wall and inlet temperatures into Equation (4.14) requires a deviation in Nu_{10} of 8 percent from the mean Nu_{10} at $T_e = 294.3^0$ K.

Nu_{10} for the present variable-property and constant-property results are compared graphically in Figures 12 and 13 with the reported experimental values of Mercer et al. [4] at inlet Reynolds numbers of 682 and 1474. The variable-property model is in excellent agreement

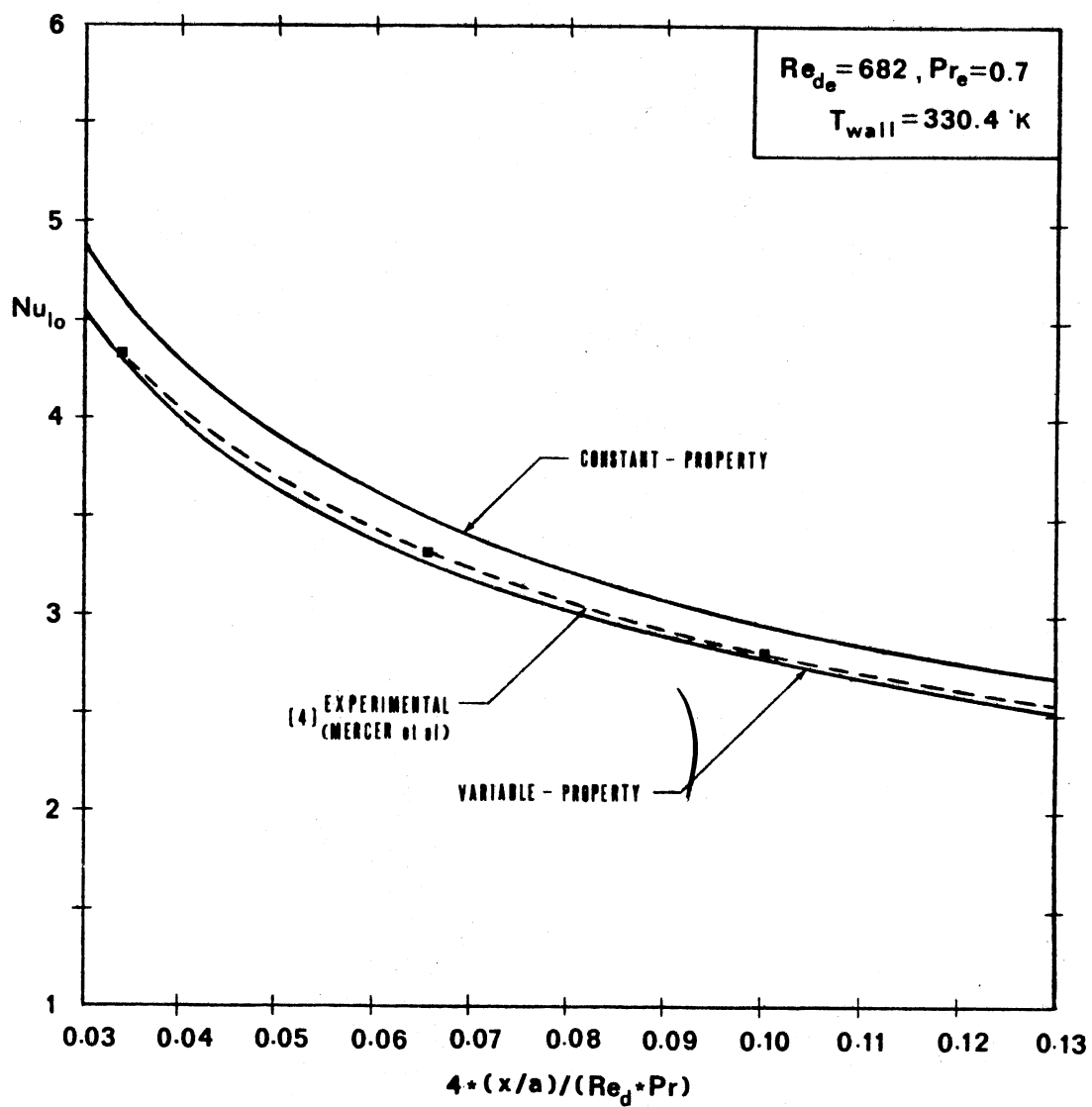


Figure 12. Comparison of Variable-Property Model with Experimental Results of [4] at Re_{de} = 682

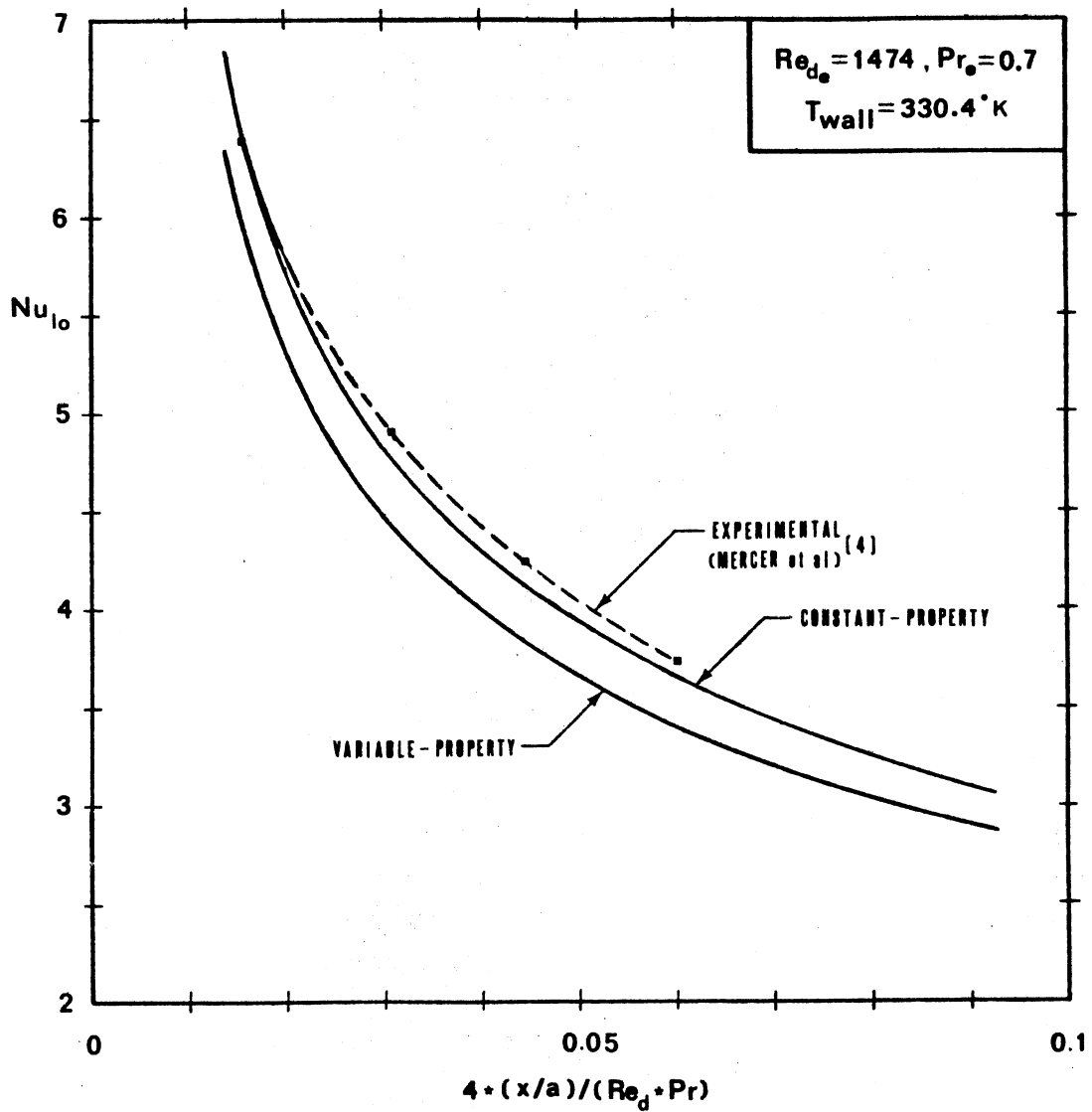


Figure 13. Comparison of Variable-Property Model with Experimental Results of [4] at $Re_{de} = 1474$

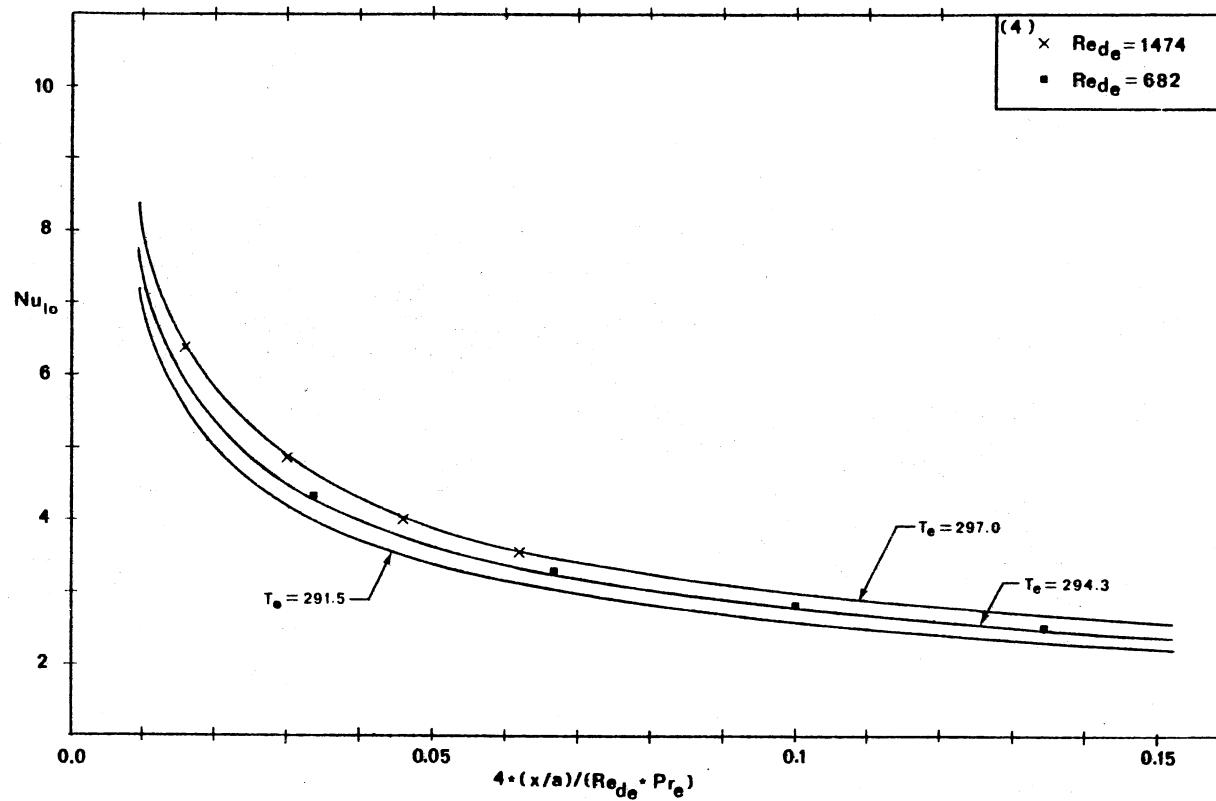


Figure 14. Variable-Property Results Shifted by Equation (4.14) with Various Inlet Temperatures

with those experimental results of [4] for air at $Re_{de} = 682$ showing a maximum deviation of 1.4 percent near $X = 0.065$. Nu_{10} differs by approximately 6 percent between the constant- and variable-property models.

Though the variable-property results agree well with those of [4] at $Re_{de} = 682$, there is an 8 percent deviation in reported values of Nu_{10} for $Re_{de} = 1474$. This suggests that either the variable-property model has failed to predict "correct" local non-dimensional heat transfer coefficients or the experimental results of [4] at $Re_{de} = 1474$ may have been based on an inlet temperature other than the mean T_e of the reported inlet temperatures. Figure 14 will be used to clarify this point.

The continuous curves in Figure 4.6 are the results from the present variable-property model. Nu_x was obtained assuming a mean inlet temperature of $294.3^{\circ}K$. Nu_x was then converted to Nu_{10} by using Equation (4.14) for the upper, lower, and mean inlet temperatures of Mercer, et al. [4]. The reported results of [4] also appear in Figure 14. If the non-dimensional variables (Re_d , Pr , Nu_{10} , Nu_x) are defined using fixed reference values (μ_e , u_e , ρ_e , C_{p_e} , k_e , h_e , or h_m) the results of both the present work and Mercer, et al. [4] should appear as a continuous curve when the non-dimensional heat transfer coefficient is plotted versus a non-dimensional entrance length.

Based on the previous discussion the deviations of [4] from a continuous curve of Nu_{10} vs X appears to be a result of inlet temperature variations between tests. If the tests for Re_{de} were performed at T_e approximately equal to $297.0^{\circ}K$ the present results would be in excellent agreement with those of Mercer, et al.

As mentioned previously the constant-property model varies from the variable-property model by approximately 6 percent for a wall-to-inlet temperature ratio of 1.1. This is a noticeable but not a significant difference in local heat transfer coefficients. But, for larger wall-to-inlet temperature ratios, sufficiently large ($T_w/T_e > 1.1$) deviations in the local heat transfer coefficients may warrant the need for a variable-property model. The effects of wall-to-inlet ratios and individual property variations on the local heat transfer coefficient will be discussed next.

4.3 Variable Property Effects

Property variations of air cause several different and opposing effects on the Nusselt number. Figures 15, 16, and 17 show the deviation from the constant-property solution that the variable-property model experiences for $T_w = 330.4, 700$ and 1000 K, respectively. The largest difference between constant- and variable-property Nu_x was located near the entrance. Table III shows the maximum and minimum percent difference between the constant- and variable-property models for the various wall temperatures.

Further investigations were performed to monitor the effects of individual property-variations on local heat transfer. This investigation was completed by holding all but one property constant for the same three wall temperatures used to produce Figures 15, 16, and 17. The inlet temperature was held constant at 294.3 K. Figures 18, 19, 20 and 21 show the effects of varying viscosity, density, thermal conductivity, and specific, respectively, on Nu_x for the three wall temperatures $330.4, 700,$ and 1000 K.

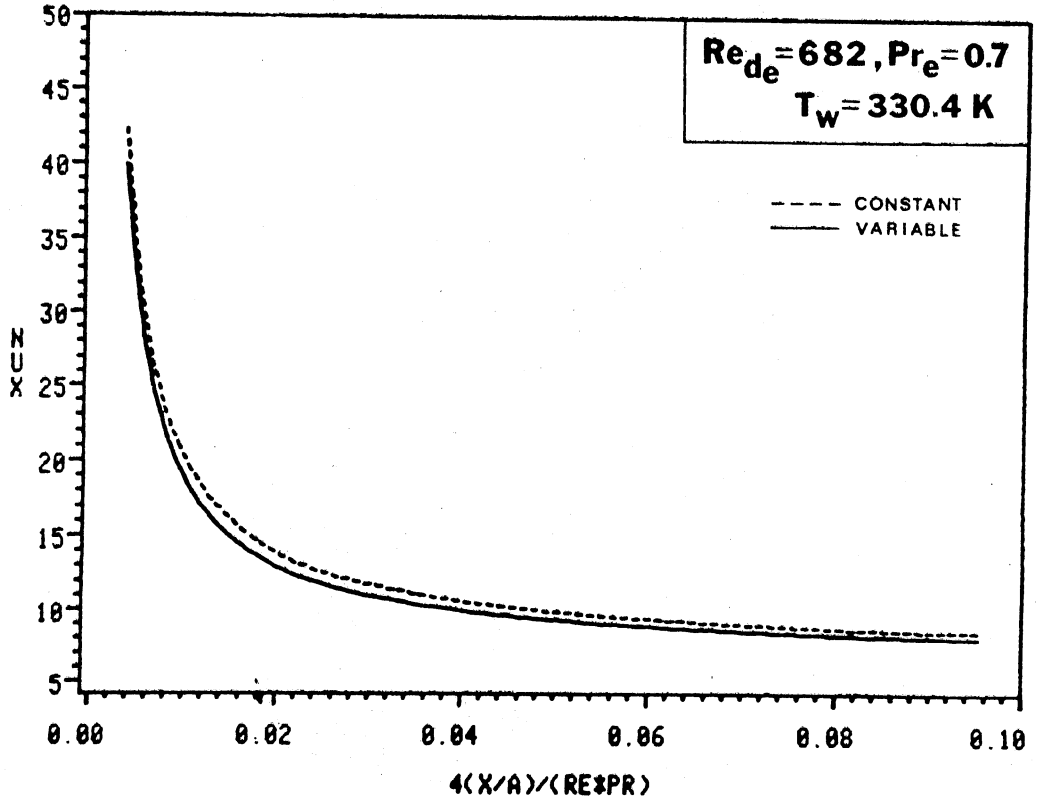


Figure 15. Constant- and Variable-Property Predictions of Nu_x at $T_w = 330.4 \text{ K}$

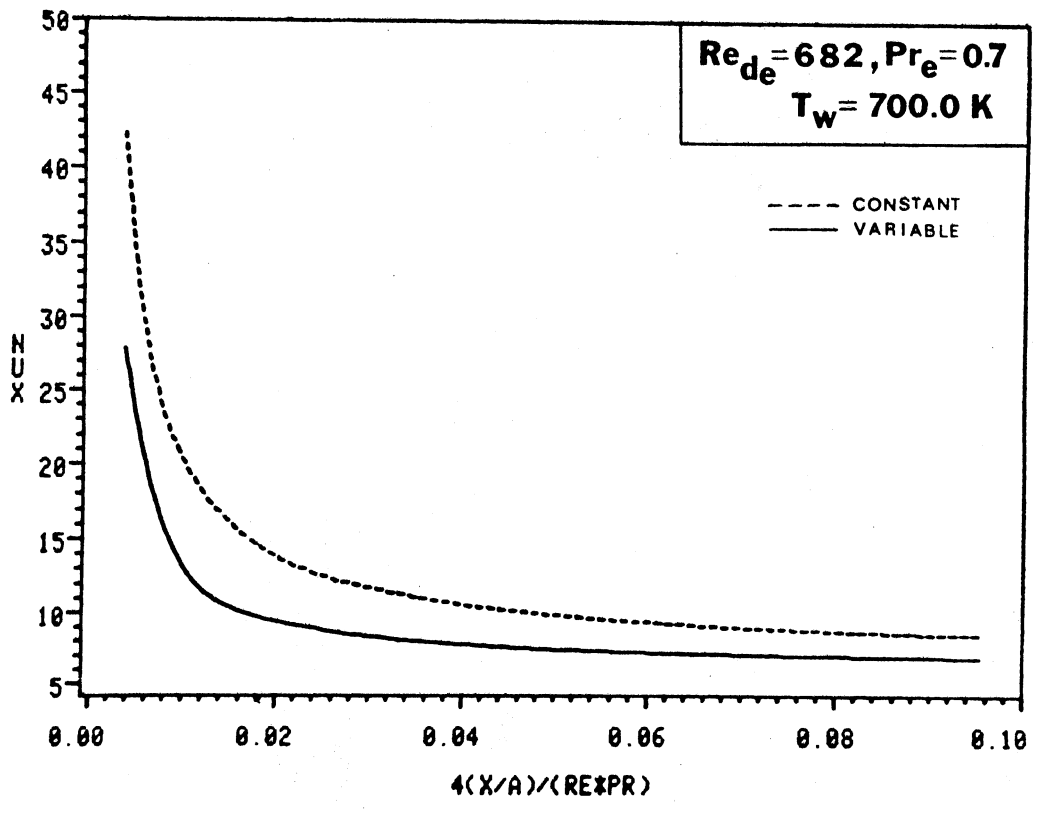


Figure 16. Constant- and Variable-Property Predictions of Nu_x at $T_w = 700 \text{ K}$

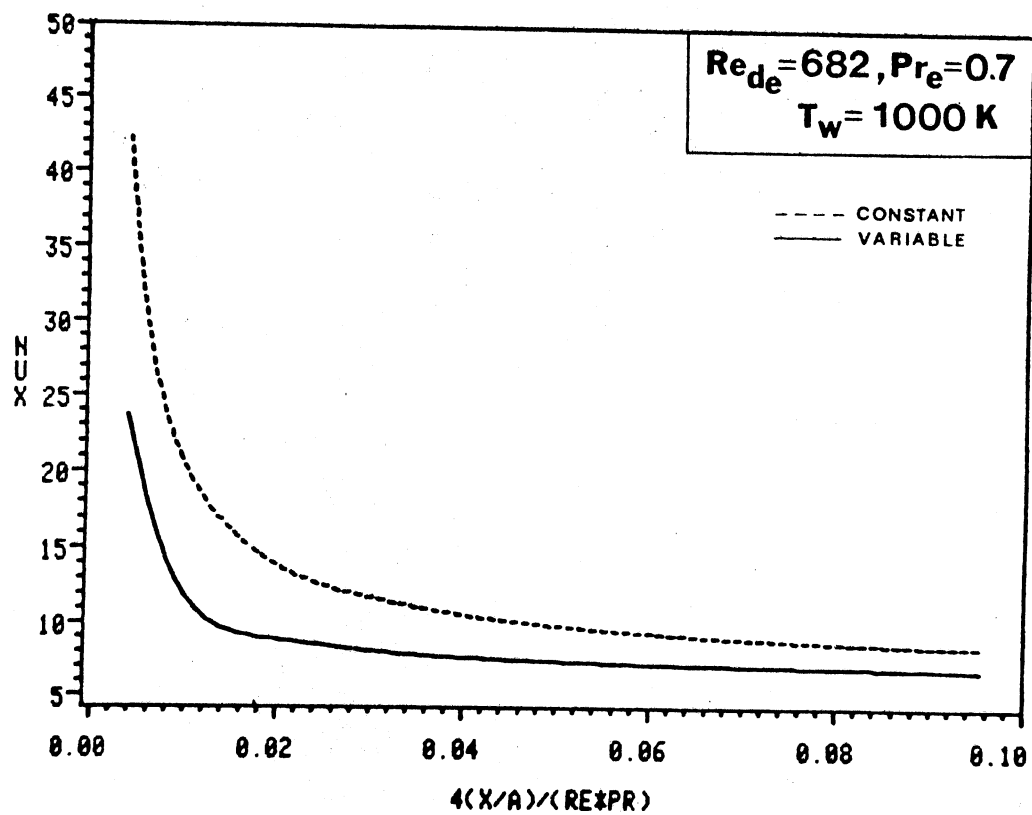


Figure 17. Constant and Variable-Property Predictions of Nu_x at $T_w = 1000 \text{ K}$

TABLE III
 PERCENT DIFFERENCE IN Nu_x BETWEEN CONSTANT- AND
 VARIABLE-PROPERTY SOLUTIONS

T_w (K)	ΔNu_x % _{max}	ΔNu_x % _{min}
330.4	7	2
700	34	9.5
1000	44	10

Figures 18 and 19 show that the general effect of viscosity and density, respectively, is a net lowering of the heat transfer coefficient for an increase in the wall temperature. Figure 20 indicates that the thermal conductivity also causes a net lowering of the heat transfer coefficient for an increase in the wall temperature. But this decrease is significantly larger than for the varying viscosity or density. The variable specific heat causes an increase in the local heat transfer coefficient as shown in Figure 21. The effect of the specific heat in increasing the local heat transfer coefficient is overcome by the tendencies of the other properties. Thus, a net lowering of the local heat transfer coefficient occurs when all properties are considered.

In summary, it appears that the most significant parameter affecting the net heat transfer coefficient is the thermal conductivity,

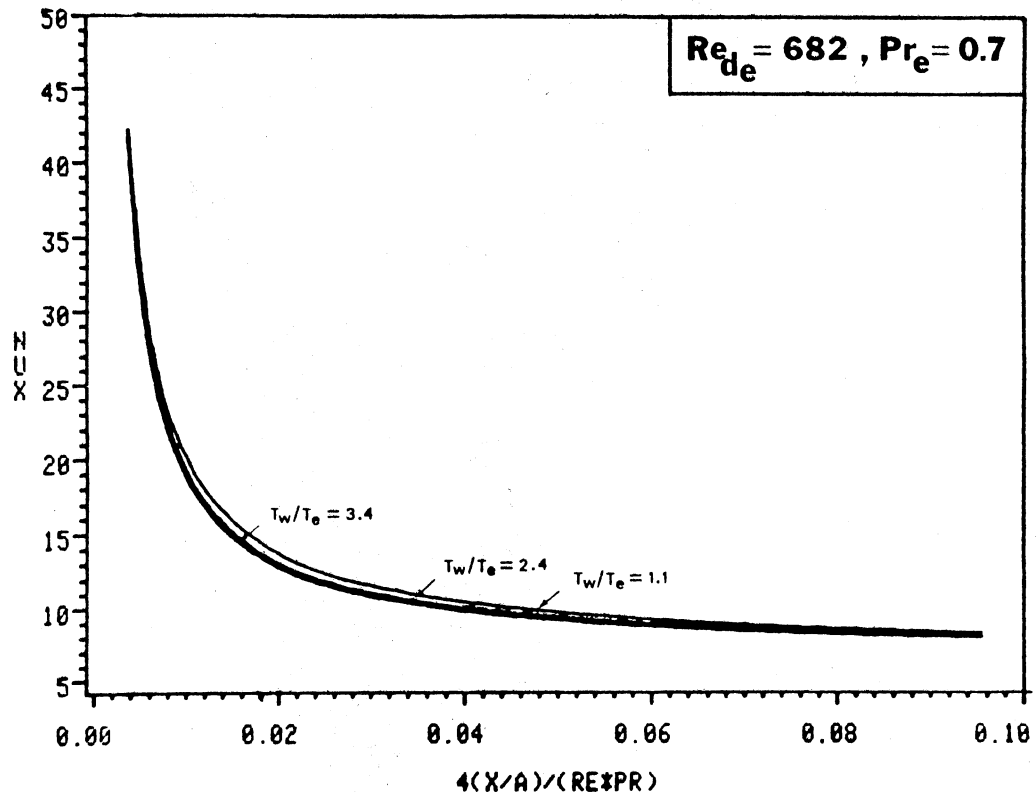


Figure 18. The Effect of Viscosity Variations on Nu_x for Various Wall-to-Inlet Temperature Ratios

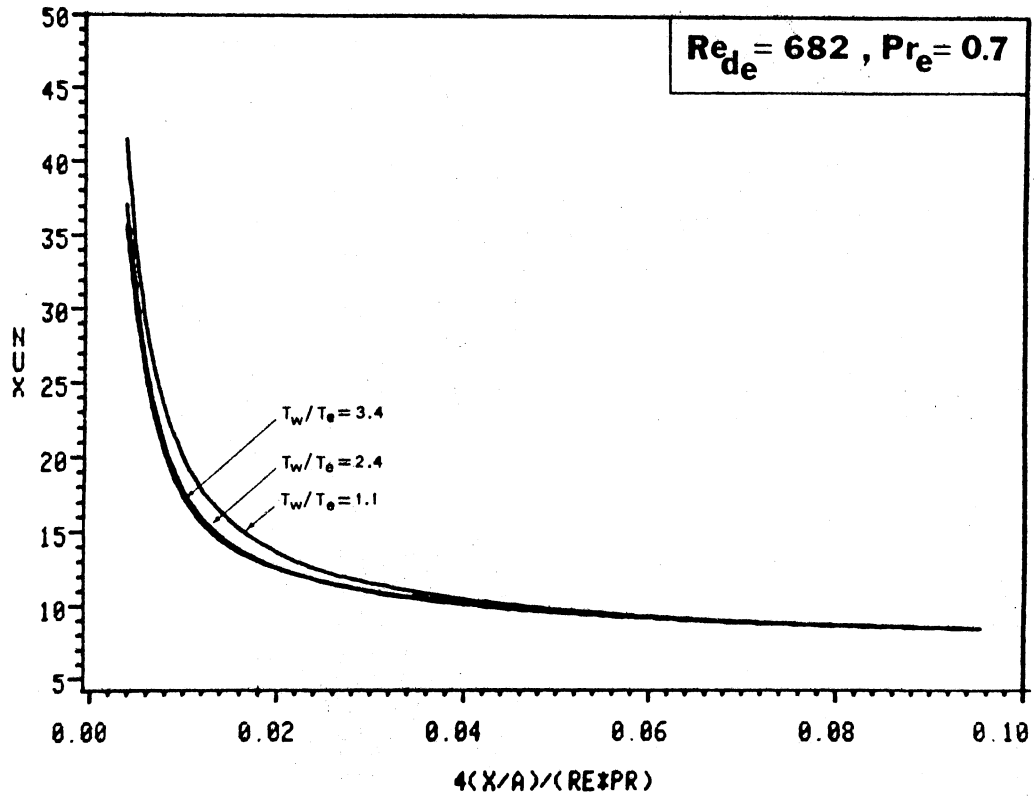


Figure 19. The Effect of Density Variations on Nu_x for Various Wall-to-Inlet Temperature Ratios

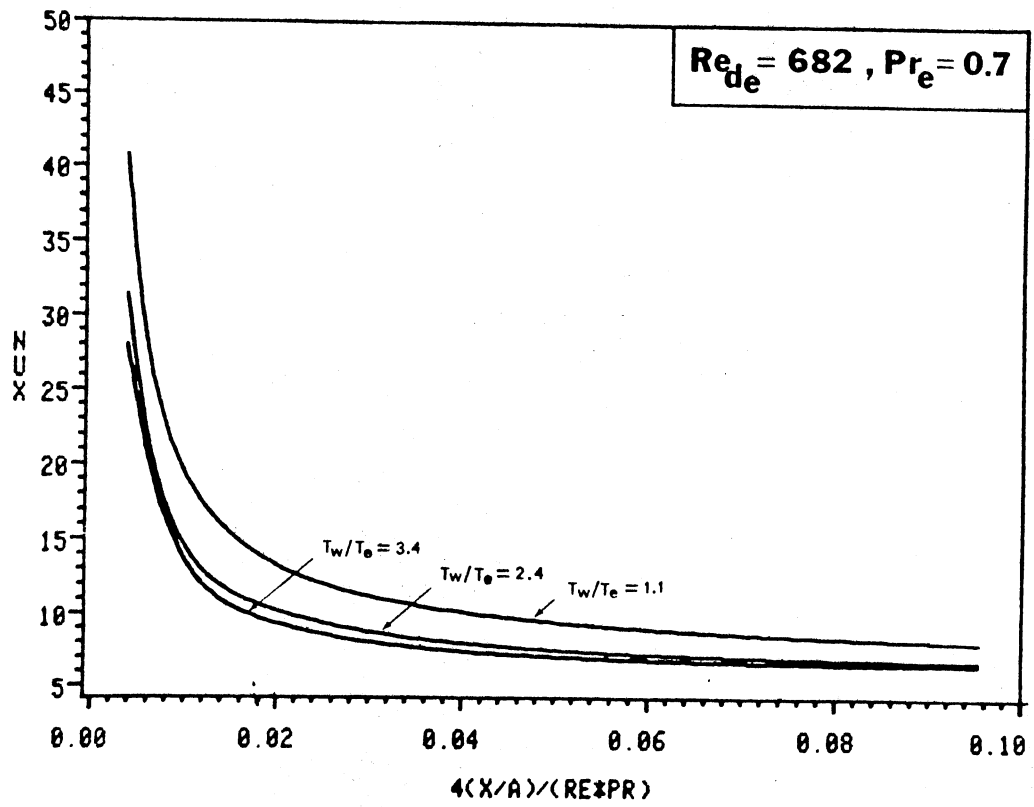


Figure 20. The Effects of Thermal Conductivity Variations on Nu_x for Various Wall to Inlet Temperature Ratios

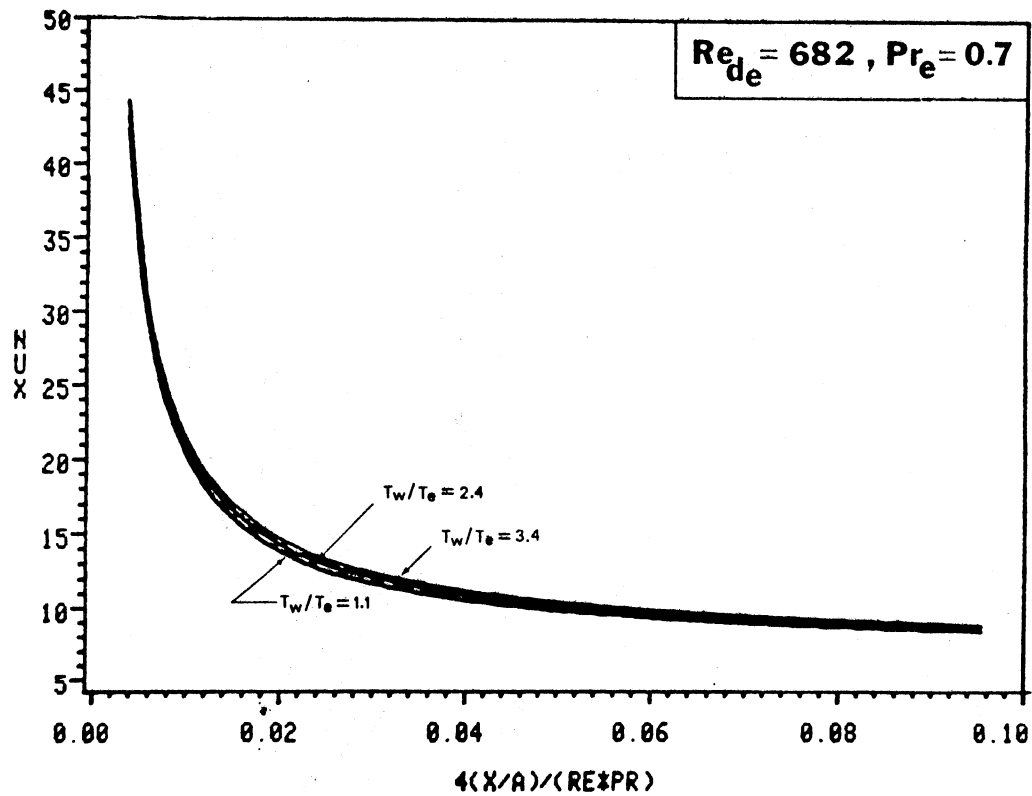


Figure 21. The Effect of Specific Heat Variations on Nu_x for Various Wall to Inlet Temperature Ratios T_w/T_e

while viscosity has little effect on altering the local heat transfer coefficient. Thus, it is important to correctly model the varying thermal conductivity when considering internal convective heat transfer for air.

4.4 Summary

The results of the present constant-property model have been shown to be in close agreement with other established constant-property models. The constant-property model also predicts the fully developed Nusselt number 7.54. The constant-property model consistently deviated from experimental results and the variable-property model was introduced in an attempt to correct these deviations.

The results of the variable-property model were in excellent agreement with experimental results of [4] for $Re_{de} = 682$; Nu_x being within 1.5 percent. The deviation from [4] for $Re_{de} = 1474$ was shown to be caused by varying inlet temperatures in the experiment of [4]. Thus, the results of the variable-property model exhibit "real", internal, convective, heat-transfer principles.

The variable-property effects were outlined in Section 4.3. There it was shown that for substantial temperature variations (i.e., $T_w/T_e > 1.1$) the constant-property model gives erroneous results. Also, by allowing only one property to vary at a time the thermal conductivity was shown to be the major factor causing a lower local heat transfer coefficient, while the viscosity was shown to exhibit the least effect on lowering the local heat-transfer coefficient.

CHAPTER V

SUMMARY, CONCLUSIONS, AND RECOMMENDATIONS

5.1 Summary and Conclusions

The accomplishments of this study may be summarized as follows:

1. The TEACH code was used as an instrument of investigation in forced convective heat transfer in the entrance region between two semi-infinite parallel plates with uniform wall temperatures.
2. Upon investigation of the constant-property model for $Pr = 0.7$, it was determined that this model was in good agreement with other more recent constant-property models. But upon comparing constant-property results with the experimental results of [4], a uniform discrepancy was noted to exist and the variable-property model outlined in Section 3.2 was introduced in an attempt to eliminate this discrepancy.
3. The variable-property model and the boundary conditions reported by [4] were implemented into the TEACH computer code. The results of the present work for Nu_x were converted by Equation (4.14) to Nu_{10} . The results obtained using the mean inlet temperature reported by [4] for $Re_{de} = 682$ were in excellent agreement with the experimental results of [4]. But when the mean inlet temperature was used again for $Re_{de} = 1474$, the present results did not match as well as the previous

case. Upon further investigation, again using Equation (4.14), the discrepancies between the present Nu_{10} and the experimentally determined Nu_{10} were attributed to the temperature variations between tests which were reported by [4].

4. In Section 4.3 a sensitivity type analysis was completed to monitor the effect that each of the physical properties (μ , ρ , C_p , and k) have on the local non-dimensionalized heat transfer coefficient. It was found that while μ and ρ cause some decrease in the local heat transfer coefficient the major contributor to this cause was found to be the thermal conductivity, k . Also, it was shown that though the specific heat does cause an increase in Nu_x , the combined effect of all the physical properties will cause a net decrease in Nu_x .

In concluding it must be noted that larger temperature gradients in the entrance region between two semi-infinite parallel plates will cause a significant decrease in Nu_x from the constant-property Nu_x . To obtain a true measure of the velocity and temperature profiles as well as the local heat transfer coefficient, a numerical model which will accurately simulate property variations is necessary.

5.2 Recommendations

As stated in the beginning of Section 2.1, the TEACH code is designed to model two-dimensional axisymmetric flow of Newtonian fluids. Because of this attribute the study of variable-property flow

for the following geometries are recommended as an extension to the present work:

1. Simple circular tube geometry.
2. Concentric tubes (annulus) geometry.
3. Sudden and smooth inlet geometries.

The application of constant wall heat flux is also recommended as an extension to the present work.

BIBLIOGRAPHY

1. Shumway, R. M., and McEligot, D. M., "Heated Laminar Gas Flow in Annuli with Temperature Dependent Transport Properties," Nucl. Sci. Eng., Vol. 46, pp. 394-407, 1971.
2. Gosman, A. D., and Pun, W. M., "Calculation of Recirculating Flows," Report No. HTS/74/2, Dept. of Mech. Engr., Imperial College, London, 1974.
3. Narang, B. S., and Hussain, N. A., "Analysis of Laminar Forced Convection Heat Transfer in the Entrance Region of a Flat Duct with Uniform Wall Temperature," ASME, Pap. 81-HT-29, 1981.
4. Mercer, W. E., Pearce, W. M., and Hitchcock, J. E., "Laminar Forced Convection in the Entrance Region Between Flat Plates," J. Heat Transfer, Vol. 89, pp. 251-257, 1967.
5. Patankar, S. V., Numerical Heat Transfer and Fluid Flow, McGraw-Hill -- Hemisphere, New York, 1980.
6. Kays, W. M., "Numerical Solutions for Laminar Flow Heat Transfer in Circular Tubes," Trans. ASME, Vol. 77, pp. 1265-1274, 1955.
7. Langhaar, H. L., "Steady Flow in the Transition Length of a Straight Tube," Trans. ASME, J. of Applied Mechanics, Vol. 64, pp. 4-55, 1942.
8. Goldberg, P., "A Digital Computer Solution for Laminar Flow Heat Transfer in Circular Tubes," M.S. Thesis, Mech. Eng. Dept., M.I.T., Cambridge, 1958.
9. Ulrichson, D. L., and Schmitz, R. A., "Laminar-Flow Heat Transfer in the Entrance Region of Circular Tubes," Int. J. Heat Mass Transfer, Vol. 8, pp. 253-258, 1965.
10. Hornbeck, R. W., "An All-Numerical Method for Heat Transfer in the Inlet of a Tube," ASME, Pap. 65-WA/HT-36, 1965.
11. Manohar, R., "Analysis of Laminar-Flow Heat Transfer in the Entrance Region of Circular Tubes," Int. J. Heat Mass Transfer, Vol. 12, pp. 15-22, 1969.
12. Kakac, S., and Özgü, M.R., "Analysis of Laminar Flow Forced Convection Heat Transfer in the Entrance Region of a Circular Pipe," Wärme-und Stoffübertragung, Bd. 2, pp. 240-245, 1969.

13. Sparrow, E. M., "Analysis of Laminar Forced-Convection Heat Transfer in the Entrance Region of Flat Rectangular Ducts," NACA Tech. Notes TN 3331, 1955.
14. Hwang, C. L., and Fan, L. T., "Finite Difference Analysis of Forced-Convection Heat Transfer in Entrance Region of Flat Rectangular Duct," Appl. Sci. Res., Sect. A 13, pp. 401-422, 1964.
15. Bankston, C. A., and McEligot, D. M., "Turbulent and Laminar Heat Transfer to Gases with Varying Properties in the Entry Region of Circular Ducts," Int. J. Heat Mass Transfer, Vol. 13, pp. 319-344, 1970.
16. Roach, P. J., Computational Fluid Dynamics, Hermosa Publishers, 1972.
17. Spalding, D. B., "A Novel Finite-Difference Formulation for Different Expressions Involving Both First and Second Derivatives," Int. Num. Methods Eng., Vol. 4, p. 551, 1972.
18. Harlow, F. H., and Welch, J.E., "Numerical Calculations of Time-Dependent Viscous Incompressible Flow of Fluid with Free Surface," Phys. Fluids, Vol. 8, pp. 2182, 1965.
19. Bergles, A. E., "Prediction of the Effects of Temperature-Dependent Fluid Properties on Laminar Heat Transfer," Low Reynolds Number Flow Heat Exchangers, (ed. Kakac, S., Shaw, R. K., and Bergles, A. E.), Hemisphere Publishing Corp., Washington, pp. 451-471, 1983.
20. Bolz, R. E., and Tuve, G. L., CRC Handbook of Tables for Applied Engineering Science, Second Edition, CRC Press, Inc., p. 651, 1976.
21. Touloukian, Y. S., and Makita, T., Thermophysical Properties of Matter, Vol. 6, p. 293, 1970.
22. Kays, W. M., and Crawford, M. E., Convective Heat and Mass Transfer, McGraw-Hill, Inc., 1980.
23. Bodia, J. R., and Osterle, J. F., "Finite Difference Analysis of Plane Poiseuille and Couette Flow Developments," App. Sci. Res., Sect. A, Vol. 10, pp. 265-276, 1961.
24. Bhatti, M. S., and Savery, C. W., "Heat Transfer in the Entrance Region of a Straight Channel: Laminar Flow with Uniform Wall Heat Flux," J. Heat Transfer, Vol. 99, pp. 142-144, 1977.
25. Narang, B. S., and Krishnamoorthy, G., "Laminar Flow in the Entrance Region of Parallel Plates," Trans. ASME, J. of Applied Mechanics, pp. 186-188, March 1976.

APPENDIX A

FLOW CHART FOR COMPUTER CODE

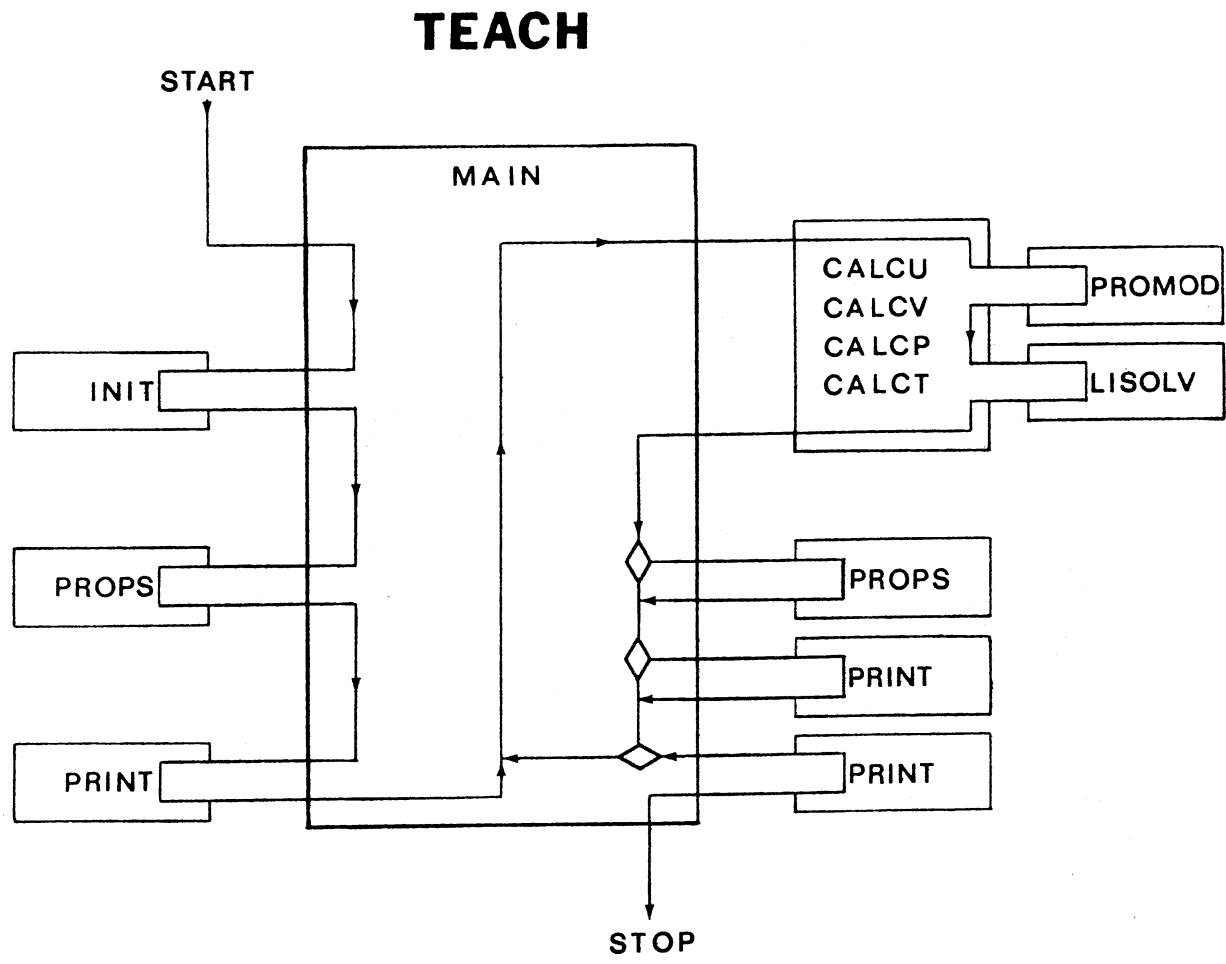


Figure 22. Flow Chart for the TEACH Code

APPENDIX B

LISTING OF COMPUTER CODE
FOR VARIABLE-PROPERTY MODEL

The program listing given here is for the variable-property case. This has been accomplished by setting the logical FORTRAN symbol INPRO equal to TRUE (i.e., INPRO = .TRUE.) (see p. 75). To obtain the constant-property model, INPRO should be set equal to FALSE (i.e., INFRO = .FALSE.)

The variable-property equations are executed in the SUBROUTINE PROPS (see p. 81). Again, to activate the SUBROUTINE PROPS the logical, function, INFRO, must be set equal to TRUE.

```

C*****
C*****
C*****          . TEACH-LAMINAR          *****
C*****          CHANEL                    *****
C***** THIS IS A COMPUTER CODE THAT SIMULATES FLOW BETWEEN *****
C***** PARALLEL PLANES. THE FLUID IS ASSUMED TO BE VISCOS *****
C***** AND HAVE VARIABLE PROPERTIES. *****
C*****
C*****
C
C
C ... A COMPUTER PROGRAM FOR THE CALCULATION OF PLANE OR AXISYMMETRIC
C ... STEADY TWO-DIMENSIONAL RECIRCULATION FLOWS.
C
C ... 1984 VERSION FOR THESIS WORK MJM, OSU, STILLWATER OKLAHOMA
C *****
C
C *** PRELIMINARIES
C
C   DIMENSION PSI(40,40),SAMPL(10),SYMBOL(11),TM(40),UA(40),ZNU(1,32)
C   CHARACTER*12 YAXES(10),XAXIS
C   COMMON
C   1/UVEL/ RESORU,NSWPU,URFU,DXEPU(32),DXPWU(32),SEWU(32)
C   1/VVEL/ RESORV,NSWPV,URFV,DYNPV(32),DYPSV(32),SNSV(32),RCV(32)
C   1/PCOR/ RESORM,NSWPP,URFP,DU(40,40),DV(40,40),IPREF,JPREF
C   1/TEMP/ RESORT,NSWPT,URFT
C   1/VAR/  U(40,40),V(40,40),P(40,40),T(40,40),PP(40,40)
C   1/ALL/  IT, JT, NI, NJ, NIM1, NJM1, GREAT
C   1/GEOM/ INDCOS, X(32), Y(32), DXEP(32), DXPW(32), DYNP(32), DYPS(32),
C   1       SNS(32), SEW(32), XU(32), YV(32), R(32), RV(32)
C   1/FLUPR/URFVIS,VISCOS,DENSIT,PRANDT,DEN(40,40),VIS(40,40),
C   1       GAMH(40,40)
C   1/KASE4/ISTEP,JSTEP,ISTP1,ISTM1,UIIN,TIN,
C   1       TWALL,SPH,TC,QWALL,JSTP1,JSTM1,FLOWIN
C
C ... NAMING THE VARIABLES THAT ARE TO BE LOGICAL
C
C   LOGICAL INCALU,INCALV,INCALP,INCALT,INPRO,WRITEU,WRITEV,WRITEP,
C   1       WRITET,PLOTET
C
C ... INPUT OF DATA NEEDED FOR LINE-PRINTER PLOTS
C
C   DATA SAMPL/1H*,1H%,1H=,1H-,1HO,1H@,1H#,1H$,1H?,1H!/
C   DATA YAXES(1),XAXIS/'NUSS      ','X/R./'(RE*PR)'/
C
C ... THESE VARIABLES DEFINE CONSTANTS USED THROUGHOUT THE PROGRAM
C
C   GREAT=1.OE30
C   NITER=0
C   LP=6
C   IT=40
C   JT=40

```

```

C
C ... GEOMETRY PARAMETERS OF THE SPECIFIED PROBLEM
C
C *** RLARGE = RADIUS OF THE DUCT
C *** DP = HALF WIDTH OF PLATE DISTANCE
C
C     DP = 0.0127
C     ALTOT = 0.60
C
C ... FLUID PROPERTIES AND BOUNDARY VALUES
C
C *** FLUID PROPERTIES
C
C     VISCOS = 1.81890373E-05
C     DENSIT = 1.1996221E+00
C     PRANDT = 7.07515885E-01
C     SPH     = 1004.339815
C
C *** THERMAL CONDUCTIVITY ::= TC = U*CP/PR
C
C     TC = 2.58251456E-02
C
C *** BOUNDARY VALUES
C
C     UIN = 0.2035569
C     TIN = 294.3
C     TWALL = 330.4
C
C *** INLET MASS FLOW
C
C     FLOWIN = UIN*DENSIT*DP
C     *****
C ... CHAPTER 1 1 1 1 1 1 PARAMETERS AND CONTROL INDICES 1 1 1 1 1 1
C     *****
C ... INDCOS DEFINES POLAR OR RECTANGULAR COORDINATE SYSTEMS
C ... (INDCOS=1; RECTANGULAR, INDCOS=2; POLAR)
C
C     INDCOS=1
C
C ... NI AND NJ DEFINE THE NUMBER OF GRID POINTS
C ...
C ...     NJ= 20 ! * * * * * * * * * * * * * * * * * * * * * * * * * * * * * * * * * !
C ...     19 ! * * * * * * * * * * * * * * * * * * * * * * * * * * * * * * * * * !
C ...     18 ! * * * * * * * * * * * * * * * * * * * * * * * * * * * * * * * * * !
C ...     17 ! * * * * * * * * * * * * * * * * * * * * * * * * * * * * * * * * * !
C ...
C ...
C ...     2 ! * * * * * * * * * * * * * * * * * * * * * * * * * * * * * * * * * !
C ...     1 ! * * * * * * * * * * * * * * * * * * * * * * * * * * * * * * * * * !
C ...
C ...     1 2 3 4 5 6 7 8 9 0 1 2 3 4 5 6 7 8 9 0 1
C ...
C ...
C ...
C
C     NI=21
C     NJ=20

```

```

      NIM1=NI-1
      NJM1=NJ-1
C
C ... THIS SECTION OF THE MAIN PROGRAM DEFINES THE GRID SYSTEM
C ... (ONLY EXPANSION ALLOWED IN THE X-DIRECTION)
C
C *** EXPR = EXPANSION RATIO OF THE GRID CELLS
C *** EXPF = EXPANSION FACTOR OF THE X-GRID CELLS
C
      EXPR = 0.9
      EXPF = 1.0+(1.0-EXPR)
      FACTOR = 0.50
      NIM2 = NIM1-1
      NIM3 = NIM2-1
100 DO 100 I=1,NIM3
      FACTOR = FACTOR + EXPF**FLOAT(I)
      FACTOR = FACTOR + (EXPF**FLOAT(NIM2))/2.
      DX = ALTOT/FACTOR
      X(1) = -0.50*DX
      DO 101 I = 2,NI
      II = I-2
101 X(I) = X(I-1)+DX*(EXPF**FLOAT(II))
C
C *** EYPR = EXPANSION RATIO FOR THE Y-GRID CELLS
C *** EYPF = EXPANSION FACTOR FOR THE Y-GRID CELLS
C
      EYPR = 1.0
      EYPF = 1.0+(1.0-EYPR)
      FACTOR = 0.50
      NJM2 = NJM1-1
      NJM3 = NJM2-1
102 DO 102 J = 1,NJM3
      FACTOR = FACTOR + EYPF**FLOAT(J)
      FACTOR = FACTOR + (EYPF**FLOAT(NJM2))/2.
      DY = DP/FACTOR
      Y(NJ) = DP+0.50*DY
      DO 103 J = 2,NJ
      JJ = J-2
      J1 = NJ - (J-1)
103 Y(J1) = Y(J1+1)-DY*(EYPF**FLOAT(JJ))
      DP = .5*(Y(NJ)+Y(NJ-1))
C
C *** PROGRAM CONTROL AND MONITOR
C
C ... MAXIT = MAXIMUM NUMBER OF ITERATIONS
C ... SORMAX = 1ST CONVERGENCE CRITERIA
C ... SORMA2 = 2ND CONVERGENCE CRITERIA
C ... IMON,JMON = I, J MONITORING LOCATIONS FOR CONVERGENCE CRITERIA
C ... INDPRI = INTERMEDIATE PRINTING AFTER INDPRI NUMBER OF ITERATIONS
C ... URFU,URFV,URFP,URFT = UNDER-RELAXATION FACTORS FOR U, V, P, AND T
C ... URFVIS = UNDER-RELAXATION FACTOR FOR VISCOSITY TERMS
C ... NSWPU,NSWPV,NSWPP,AND NSWPT = NUMBER OF SWEEPS FOR THE U,V,P,AND T
C ... FIELDS WITH THE USE OF A TDMA.
C ... INCAL( ): DECISION TO COMPUTE U,V,P,OR T FIELDS.
C ... WRITE( ): DECISION TO WRITE U,V,P,OR T FIELDS.
C ... PLOTTER: DECISION TO PLOT

```

```

C ... INPRO : DECISION TO UPDATE PROPERTIES
C
  MAXIT = 250
  SORMAX=1.OE-05
  SORMA2=SORMAX*3.
  IMON=6
  JMON=6
  INDPRI=1000
  NUMPRI=1
  URFU=0.39
  URFV=0.39
  URFI=1.0
  URFT=0.9
  URFVIS=1.0
  NSWPU = 1
  NSWPV = 1
  NSWPP = 3
  NSWPT = 1
  INCALU = .TRUE.
  INCALV = .TRUE.
  INCALP = .TRUE.
  INCALT = .TRUE.
  WRITEU = .FALSE.
  WRITEV = .FALSE.
  WRITEP = .FALSE.
  WRITET = .FALSE.
  PLOTET = .FALSE.
  INPRO = .TRUE.

C
C *****
C CHAPTER 2 2 2 2 2 2 INITIAL OPERATIONS 2 2 2 2 2 2 2 2 2 2 2 2
C *****
C ... CALCULATE GEOMETRICAL QUANTITIES AND SET VARIABLES TO ZERO
C
  CALL INITIAL
C
C ... INITIALIZE VARIABLE FIELDS
C
C ... THIS IS USED TO SETUP THE UNIFORM INLET VELOCITY.
C
  DO 200 J=2,NJM1
    U(2,J) = UIN
  200 T(1,J) = TIN
  DO 201 I = 2,NIM1
    T(I,NJ) = TWALL
  201 FACTOR = 1.0
  DO 202 I = 2,NI
    DO 202 J = 2,NJM1
      IF (I.NE.NI) T(I,J) = TWALL/2.
  202 IF (I.NE.2) U(I,J) = FACTOR*UIN
C
C ... PREF IS A REFERENCE PRESSURE USED TO INITIALIZE A GRID PRESSURE
C ... SINCE ALL BOUNDARY VELOCITIES ARE KNOWN. PROGRAM COMPUTES
C ... PRESSURE FIELD (ACTUALLY DELTA P IS THE ONLY IMPORTANT PARAMETER.)

```

```

C
  PREF = 101.325
  IPREF = 2
  JPREF = 5
  DO 2000 I = 1,NIM1
  DO 2000 J = 2,NJM1
2000 P(I,J) = PREF
C
C ... CHANGE ANY FLUID PROPERTIES DUE TO NODE TEMPERATURE CHANGES
C
  IF (INPRO)CALL PROPS
C
C ... INITIAL OUTPUT
C
  WRITE(LP,203)
203  FORMAT(///1H ,120(1H*)///)
  WRITE(LP,204)
  WRITE(LP,205)UIN
205  FORMAT(///1H ,15X,'AVRAGE INLET FLUID VELOCITY ' ,
1T60,1H=,3X,1PE11.3)
  RE = 4.*DP*UIN*DENSIT/VISCOS
  WRITE(LP,206)RE
206  FORMAT(1H ,15X,'REYNOLDS NUMBER',T60,1H=,3X,1PE11.3)
  WRITE(LP,207)PRANDT
207  FORMAT(1H ,15X,'PRANDTL NUMBER ' ,T60,1H=,3X,1PE11.3)
  WRITE(LP,208)VISCOS
208  FORMAT (1H ,15X,'FLUID VISCOSITY',T60,1H=,3X,1PE11.3)
  WRITE(LP,209)DENSIT
209  FORMAT(1H ,15X,'FLUID DENSITY',T60,1H=,3X,1PE11.3)
  WRITE(LP,211) ALTOT
211  FORMAT(1H ,15X,'LENGTH OF DUCT',T60,1H=,3X,1PE11.3)
  WRITE(LP,212) DP,EXPF,EYPF
212  FORMAT(1H ,15X,'1/2 WIDTH OF CHANNEL',T60,1H=,3X,1PE11.3/
11H ,15X,'X-GRID EXPANSION FACTOR',T60,1H=,3X,1PE11.3/
11H ,15X,'Y-GRID EXPANSION FACTOR',T60,1H=,3X,1PE11.3)
  WRITE(LP,210)TIN,TWALL
210  FORMAT (1H ,15X,'TEMPERATURE BOUNDARY CONDITIONS ARE'//
11H ,25X,'INLET TEMPERATURE',T60,1H=,3X,1PE11.3/
11H ,25X,'WALL TEMPERATURE',T60,1H=,3X,1PE11.3)
  WRITE(LP,203)
  IF (WRITEU) CALL PRINT(2,2,NI,NJ,IT,JT,XU,Y,U,'UVEL')
  IF (WRITEV) CALL PRINT(2,2,NI,NJ,IT,JT,X,YV,V,'VVEL')
  IF (WRITEP) CALL PRINT(2,2,NI,NJ,IT,JT,X,Y,P,'PRES')
  IF (WRITET) CALL PRINT(2,2,NI,NJ,IT,JT,X,Y,T,'TEMP')
C
*****
C 3 3 3 3 3 3 3 3 3 CHAPTER 3 3 3 3 3 3 3 3 3 3 3
C *****
  WRITE(LP,310) IMON,JMON
300  NITER=NITER+1
C
C ... UPDATE MAIN DEPENDENT VARIABLES
C
  IF (INCALU) CALL CALCU
  IF (INCALV) CALL CALCV
  IF (INCALP) CALL CALCP
  IF (INCALT) CALL CALCT

```



```

C
C ... UPDATE FLUID PROPERTIES
C
      IF (INPRO) CALL PROPS
      WRITE(LP,311)NITER,RESORU,RESORV,RESORM,RESORT,U(IMON,JMON),
1      V(IMON,JMON),P(IMON,JMON),T(IMON,JMON)
      IF (MOD(NITER,INDPRI).NE.O) GOTO 301
      IF (WRITEU) CALL PRINT(2,2,NI,NJ,IT,JT,XU,Y,U,'UVEL')
      IF (WRITEV) CALL PRINT(2,2,NI,NJ,IT,JT,X,YV,V,'VVEL')
      IF (WRITEP) CALL PRINT(2,2,NI,NJ,IT,JT,X,Y,P,'PRES')
      IF (WRITET) CALL PRINT(2,2,NI,NJ,IT,JT,X,Y,T,'TEMP')
C
C ... PRINTOUT THE MONITOR LOCATION
C
      WRITE(LP,310)IMON,JMON
301 CONTINUE
C
C ... TERMINATION TESTS
C
      IF(NITER.EQ.MAXIT)GO TO 302
      IF(NITER.EQ.100.AND.RESORM.GT.1.OE4*SORMAX) GO TO 302
      IF (RESORT.GT.SORMAX) GOTO 300
      IF (RESORU.GT.SORMA2.OR.RESORM.GT.SORMAX) GOTO 300
302 CONTINUE
C
C *****
C CHAPTER 4 4 4 4 FINAL OPERATIONS AND OUTPUT 4 4 4 4
C *****
C
      IF (INCALU) CALL PRINT(2,2,NI,NJ,IT,JT,XU,Y,U,'UVEL')
      IF (INCALV) CALL PRINT(2,2,NI,NJ,IT,JT,X,YV,V,'VVEL')
      IF (INCALP) CALL PRINT(2,2,NI,NJ,IT,JT,X,Y,P,'PRES')
      IF (INCALT) CALL PRINT(2,2,NI,NJ,IT,JT,X,Y,T,'TEMP')
      CALL PRINT(2,2,NI,NJ,IT,JT,X,Y,VIS,'VISC')
C
C ... COMPUTATIONS FOR SOME OF THE FINIAL OUTPUT PARAMETERS
C ... (NUSSLET NUMBER, FRICTION COEFFICIENTS, ETC.)
C
      DUU=DENSIT*UIN*UIN
      DY = YV(NJ) - Y(NUM1)
      ANI = 0.0
      X(1) = 4.*(X(1)/DP)/(RE*PRANDT)
      WRITE(LP,420)
      DO 410 I=2,NIM1
      X(I) = 4.*(X(I)/DP)/(RE*PRANDT)
      SUMT=0.0
      SAVG=0.0
      DTDX = (T(I+1,NJ)-T(I-1,NJ))/(SEW(I)*2.0)
      DO 411 J = 2,NUM1
      UAVG = (U(I,J)+U(I+1,J))/2.
C
C ... THE INTEGRAL OF UTDY
C
      SUMT = SUMT + T(I,J)*UAVG*SNS(J)
C
C ... THE INTEGRAL OF UDY

```

```

C
411 SAVG = SAVG + UAVG*SNS(J)
    UA(I) = SAVG/DP
    TM(I) = SUMT/(UA(I)*DP)
    AN1 = (TWALL-T(I,NUM1))/DY
C
C ... THE NUSSELT NUMBER, NUX = ANU
C
    ANU = 4.*DP*AN1/(TWALL-TM(I))
C
C ... ANI = THE SUM OF NUX*DX
C ... ANM = NUX*DX/(X+) = THE MEAN NUSSELT NUMBER
C
    DELX = (X(I+1)-X(I-1))/2.
    ANI = ANI + ANU*DELX
    ANM = ANI/X(I-1)
    SSC = VISCOS*(-U(I,NUM1))/(DY*DUU)
    DTDY = AN1
    DUDY = U(I,NUM1)/DY
    WRITE(LP,430) I, X(I), ANU, ANM, TM(I), XU(I), SSC
C
410 CONTINUE
C
C ... PLOT QUANTITIES REQUIRED
C
    IF(PLOTTER) CALL PLOT(X,32,NIM2,XAXIS,ZNU,1,1,YAXES,
1      SAMPL,LP,ID)
C
C ... THIS PART OF THE MAIN CODE MAKES SOME SUPPLEMENTARY PLOTS
C ... OF THE NONDIMENSIONAL MEAN TEMPERATURE ...
C ... THETA MEAN = (TO-TM)/(TO-TE)
C
    DO 450 I = 2,NIM1
450  ZNU(1,I-1) = (TWALL-TM(I))/(TWALL-TIN)
    YAXES(1) = 'THETA MEAN'
    IF(PLOTTER) CALL PLOT(X,32,NIM2,XAXIS,ZNU,1,1,YAXES,SAMPL,LP,ID)
    STOP
C
C ... FORMAT STATEMENTS
C
204  FORMAT(1H ,5X, '(CHANEL VARB1.F) LAMINAR FLOW THROUGH A CHANNEL'
1, ' WITH CONSTANT TEMPERATURE BOUNDARIES (EXPANDING X-GRID SYSTEM)'
2////)
C ...
310  FORMAT(///1H , 'ITER   I-----ABSOLUTE RESIDUAL SOURCE SUMS',
1'-----I           I-----FIELD VALUES AT MONITORING LOCATION',
1' (',I2,',',I2,')', '-----I//2X, 'NO.',3X, 'UMOM',6X, 'VMOM',6X,
1' MASS',6X, 'ENER',31X, 'U',9X, 'V',9X, 'P',9X, 'T'
1, '          ',9X, '          '//)
C ...
311  FORMAT(1H ,I3,3X,1P4E10.3,25X,1P4E10.3)
C ...
420  FORMAT(////1H , 'DISTRIBUTION OF NUSSELT NUMBER AND SHEAR-STRESS'
1, ' COEFFICIENT ALONG THE WALL'//1H ,1X,1HI,10X,1HX,8X,
2'  NUX          ',2X, '  NUM          ',4X, 'MEAN TEMP.',5X, 'XU',
36X, 'S.S. COEFF.'//)

```



```

C
  ARDEN=0.0
  FLOW=0.0
  DO 204 J=2,NJM1
    DENAR=0.5*(DEN(NIM1,J)+DEN(NIM1-1,J))*SNS(J)
    ARDEN=ARDEN+DENAR
204  FLOW=FLOW+DENAR*U(NIM1,J)
    UINC=(FLOWIN-FLOW)/ARDEN
    DO 205 J=2,NJM1
205  U(NI,J) = U(NIM1,J)+UINC
C
C ... SYMMETRY AXIS (DU/DY = 0.0)
C
  J = 2
  DO 206 I = 3,NIM1
206  AS(I,J) = 0.0
  RETURN
C
C *****
C CHAPTER 3 3 3 3 3 3 V MOMENTUM 3 3 3 3 3 3 3
C *****
C
C ENTRY MODV
C
C ... SYMETRY AXIS
C
  DO 302 I=2,NI
302  AS(I,3)=0.0
  RETURN
C
C *****
C CHAPTER 4 4 4 4 4 PRESSURE CORRECTION 4 4 4 4 4 4 4
C *****
C
C ENTRY MODP
C
C ... NO MODIFICATIONS WITH VELOCITIES SPECIFIED AT BOUNDARIES.
C
  RETURN
C
C *****
C CHAPTER 5 5 5 5 5 THERMAL ENERGY 5 5 5 5 5 5 5
C *****
C
C ENTRY MODT
C
C ... LARGE DUCT WALL
C
  DY = YV(NJ) - Y(NJM1)
  J=NJM1
  DO 502 I=2,NIM1
    AN(I,J) = 0.0
    TERM=GAMH(I,J)*SEW(I)/DY
    SU(I,J)=SU(I,J)+TERM*TWALL
502  SP(I,J)=SP(I,J)-TERM
C

```

```

C ... SYMETRY AXIS
C
DO 503 I=2,NIM1
503 AS(I,2)=0.0
C
C ... OUTLET CONDITIONS (NORMAL GRADIENT IS ZERO.)
C
I = NIM1
DO 504 J = 2,NJM1
504 AE(I,J) = 0.0
RETURN
END
C
C *****
SUBROUTINE PROPS
C *****
C *****
CHAPTER 0 0 0 0 PRELIMINARIES 0 0 0 0 0
C *****
C *****
COMMON
1/VAR/ U(40,40),V(40,40),P(40,40),T(40,40),PP(40,40)
1/FLUPR/URFVIS,VISCOS,DENSIT,PRANDT,DEN(40,40),VIS(40,40),
1 GAMH(40,40)
1/ALL/ IT,JT,NI,NJ,NIM1,NJM1,GREAT
1/KASE4/ISTEP,JSTEP,ISTP1,ISTM1,UIN,TIN,
1 TWALL,SPH,TC,QWALL,JSTP1,JSTM1,FLOWIN
C
C *****
CHAPTER 1 1 DENSITY, AND THERMAL EXCAHNGE COEFFICIENT 1 1 1
C *****
C ... PROPERTIES WILL VARY WITH TEMPERATURE
C
DO 100 I = 2,NIM1
DO 100 J = 2,NJM1
TPOW = T(I,J)**1.5
CONST= 245.4*(10.**(-12./T(I,J)))
VIS(I,J) = (1.458E-06*TPOW)/(T(I,J)+110.4)
COND = 4186.*(6.325E-07*TPOW)/(T(I,J)+CONST)
DEN(I,J) = P(I,J)*1000./(T(I,J)*287.0)
IF (T(I,J).LT.600.) CP = 4184.*( .244388-4.20419E-05*T(I,J)+
*9.611283E-08*T(I,J)**2-1.16383E-11*T(I,J)**3)
IF (T(I,J).GE.600.) CP = 4184.*( .208831+7.71027E-05*T(I,J)-
*8.56726E-09*T(I,J)**2-4.75772E-12*T(I,J)**3)
100 GAMH(I,J) = COND/CP
RETURN
END

```

```

C ... START OF SF4.FOR
C
C     SUBROUTINE INITIAL
C
C     *****
C     CHAPTER 0 0 0 0 0 PRELIMINARIES 0 0 0 0 0 0 0 0
C     *****
C
C     COMMON
1/UVEL/ RESORU,NSWPU,URFU,DXEPU(32),DXPWU(32),SEWU(32)
1/VVEL/ RESORV,NSWPV,URFV,DYNPV(32),DYPSV(32),SNSV(32),RCV(32)
1/PCOR/ RESORM,NSWPP,URFP,DU(40,40),DV(40,40),IPREF,JPREF
1/TEMP/ RESORT,NSWPT,URFT
1/VAR/  U(40,40),V(40,40),P(40,40),T(40,40),PP(40,40)
1/ALL/  IT, JT, NI, NJ, NIM1, NJM1, GREAT
1/GEOM/ INDCOS, X(32), Y(32), DXEP(32), DXPW(32), DYNP(32), DYPS(32),
1      SNS(32), SEW(32), XU(32), YV(32), R(32), RV(32)
1/FLUPR/URFVIS,VISCOS,DENSIT,PRANDT,DEN(40,40),VIS(40,40),
1      GAMH(40,40)
1/COEF/ AP(40,40),AN(40,40),AS(40,40),AE(40,40),AW(40,40),
1      SU(40,40),SP(40,40)
1/KASE4/ISTEP,JSTEP,ISTP1,ISTM1,UIIN,TIN,
1      TWALL,SPH,TC,QWALL,JSTP1,JSTM1,FLOWIN
C     *****
C     CHAPTER 1 1 1 1 1 CALCULATE GEOMETRICAL QUANTITIES 1 1 1 1
C     *****
C
C     NIM1=NI-1
C     NJM1=NJ-1
C     DO 100 J=1,NJ
C     R(J)=Y(J)
100 IF(INDCOS.EQ.1)R(J)=1.0
C     DXPW(1)=0.0
C     DXEP(NI)=0.0
C     DO 101 I=1,NIM1
C     DXEP(I)=X(I+1)-X(I)
101 DXPW(I+1)=DXEP(I)
C     DYPS(1)=0.0
C     DYNP(NJ)=0.0
C     DO 102 J=1,NJM1
C     DYNP(J)=Y(J+1)-Y(J)
102 DYPS(J+1)=DYNP(J)
C     SEW(1)=0.0
C     SEW(NI)=0.0
C     DO 103 I=2,NIM1
103 SEW(I)=0.5*(DXEP(I)+DXPW(I))
C     SNS(1)=0.0
C     SNS(NJ)=0.0
C     DO 104 J=2,NJM1
104 SNS(J)=0.5*(DYNP(J)+DYPS(J))
C     XU(1)=0.0
C     DO 105 I=2,NI

```

```

105 XU(I)=0.5*(X(I)+X(I-1))
    DXPWU(1)=0.0
    DXPWU(2)=0.0
    DXEPU(1)=0.0
    DXEPU(NI)=0.0
    DO 106 I=2,NIM1
106 DXEPU(I)=XU(I+1)-XU(I)
    DXPWU(I+1)=DXEPU(I)
    SEWU(1)=0.0
    SEWU(2)=0.0
    SEWU(NI)=0.0
    DO 107 I=3,NIM1
107 SEWU(I)=0.5*(DXEPU(I)+DXPWU(I))
    YV(1)=0.0
    RV(1)=0.0
    DO 108 J=2,NJ
    RV(J)=0.5*(R(J)+R(J-1))
    RCV(J)=0.5*(RV(J)+RV(J-1))
108 YV(J)=0.5*(Y(J)+Y(J-1))
    DYPSV(1)=0.0
    DYPSV(2)=0.0
    DYNP(NI)=0.0
    DO 109 J=2,NJM1
    DYNPV(J)=YV(J+1)-YV(J)
109 DYPSV(J+1)=DYNPV(J)
    SNSV(1)=0.0
    SNSV(2)=0.0
    SNSV(NJ)=0.0
    DO 110 J=3,NJM1
110 SNSV(J)=0.5*(DYNPV(J)+DYPSV(J))
C
C *****
C CHAPTER 2 2 2 2 2 2 SET VARIABLES TO ZERO 2 2 2 2 2 2
C *****
C
    DO 200 I=1,NI
    DO 200 J=1,NJ
    U(I,J)=0.0
    V(I,J)=0.0
    P(I,J)=0.0
    PP(I,J)=0.0
    DEN(I,J)=DENSIT
    VIS(I,J)=VISCOS
    GAMH(I,J) = VISCOS/PRANDT
    DU(I,J)=0.0
    DV(I,J)=0.0
    SU(I,J)=0.0
    SP(I,J)=0.0
200 T(I,J)=0.0
    RETURN
    END
C
C
C SUBROUTINE CALCU
C
C *****

```

```

C      CHAPTER 0 0 0 0 0 PRELIMINARIES 0 0 0 0 0 0 0 0 0 0
C      *****
C
C      COMMON
1/UVEL/ RESORU,NSWPU,URFU,DXEPU(32),DXPWU(32),SEWU(32)
1/PCOR/ RESORM,NSWPP,URFP,DU(40,40),DV(40,40),IPREF,JPREF
1/VAR/  U(40,40),V(40,40),P(40,40),T(40,40),PP(40,40)
1/ALL/  IT,JT,NI,NJ,NIM1,NJM1,GREAT
1/GEOM/ INDCOS,X(32),Y(32),DXEP(32),DXPW(32),DYNP(32),DYPS(32),
1      SNS(32),SEW(32),XU(32),YV(32),R(32),RV(32)
1/FLUPR/URFVIS,VISCOS,DENSIT,PRANDT,DEN(40,40),VIS(40,40),
1      GAMH(40,40)
1/COEF/ AP(40,40),AN(40,40),AS(40,40),AE(40,40),AW(40,40),
1      SU(40,40),SP(40,40)
C
C      *****
C      CHAPTER 1 1 1 1 ASSEMBLY OF COEFFICIENTS 1 1 1 1 1 1
C      *****
C
C      DO 100 I=3,NIM1
C      DO 101 J=2,NJM1
C
C      ... COMPUTE AREAS AND VOLUME
C
C      AREAN=RV(J+1)*SEWU(I)
C      AREAS=RV(J)*SEWU(I)
C      AREAEW=R(J)*SNS(J)
C      VOL=R(J)*SEWU(I)*SNS(J)
C
C      ... CALCULATE CONVECTION COEFFICIENT
C
C      GN=0.5*(DEN(I,J+1)+DEN(I,J))*V(I,J+1)
C      GNW=0.5*(DEN(I-1,J)+DEN(I-1,J+1))*V(I-1,J+1)
C      GS=0.5*(DEN(I,J-1)+DEN(I,J))*V(I,J)
C      GSW=0.5*(DEN(I-1,J)+DEN(I-1,J-1))*V(I-1,J)
C      GE=0.5*(DEN(I+1,J)+DEN(I,J))*U(I+1,J)
C      GP=0.5*(DEN(I,J)+DEN(I-1,J))*U(I,J)
C      GW=0.5*(DEN(I-1,J)+DEN(I-2,J))*U(I-1,J)
C      CN=0.5*(GN+GNW)*AREAN
C      CS=0.5*(GS+GSW)*AREAS
C      CE=0.5*(GE+GP)*AREAEW
C      CW=0.5*(GP+GW)*AREAEW
C
C      ... CALCULATE DIFFUSION COEFFICIENTS
C
C      VISN=0.25*(VIS(I,J)+VIS(I,J+1)+VIS(I-1,J)+VIS(I-1,J+1))
C      VISS=0.25*(VIS(I,J)+VIS(I,J-1)+VIS(I-1,J)+VIS(I-1,J-1))
C      DN=VISN*AREAN/DYNP(J)
C      DS=VISS*AREAS/DYPS(J)
C      DE=VIS(I,J)*AREAEW/DXEPU(I)
C      DW=VIS(I-1,J)*AREAEW/DXPWU(I)
C
C      ... CALCULATE COEFFICIENTS OF SOURCE TERMS
C
C      SMP=CN-CS+CE-CW
C      CP=AMAX1(0.0,SMP)

```



```

CPO=CP
C
C ... ASSEMBLE MAIN COEFFICIENTS
C
AN(I,J)=AMAX1(ABS(O.5*CN),DN)-O.5*CN
AS(I,J)=AMAX1(ABS(O.5*CS),DS)+O.5*CS
AE(I,J)=AMAX1(ABS(O.5*CE),DE)-O.5*CE
AW(I,J)=AMAX1(ABS(O.5*CW),DW)+O.5*CW
DU(I,J)=AREA*EW
SU(I,J)=CPO*U(I,J)+DU(I,J)*(P(I-1,J)-P(I,J))
SP(I,J)=-CP
101 CONTINUE
100 CONTINUE
C
C *****
C CHAPTER 2 2 2 2 PROBLEM MODIFICATION 2 2 2 2 2 2
C *****
C
CALL MODU
C
CHAPTER 3 FINIAL COEFF. ASSEMBLY & RESIDUAL SOURCE CALCULATION
C
RESORU=0.0
DO 300 I=3,NIM1
DO 301 J=2,NJM1
AP(I,J)=AN(I,J)+AS(I,J)+AE(I,J)+AW(I,J)-SP(I,J)
DU(I,J)=DU(I,J)/AP(I,J)
RESOR=AN(I,J)*U(I,J+1)+AS(I,J)*U(I,J-1)+AE(I,J)*U(I+1,J)+
1 AW(I,J)*U(I-1,J)-AP(I,J)*U(I,J)+SU(I,J)
VOL=R(J)*SEW(I)*SNS(J)
SORVOL=GREAT*VOL
IF(-SP(I,J).GT.O.5*SORVOL)RESOR=RESOR/SORVOL
RESORU=RESORU+ABS(RESOR)
C
C ... UNDER RELAXATION
C
AP(I,J)=AP(I,J)/URFU
SU(I,J)=SU(I,J)+(1.-URFU)*AP(I,J)*U(I,J)
DU(I,J)=DU(I,J)*URFU
301 CONTINUE
300 CONTINUE
C
C *****
C CHAPTER 4 4 4 4 SOLUTION OF DIFFERENCE EQUATION 4 4 4 4
C *****
C
DO 400 N=1,NSWPU
400 CALL LISOLV(3,2,NI,NJ,IT,JT,U)
RETURN
END
C
SUBROUTINE CALCV
C
COMMON
1/VVEL/ RESORV,NSWPV,URFV,DYNPV(32),DYPSV(32),SNSV(32),RCV(32)
1/PCOR/ RESORM,NSWPP,URFP,DU(40,40),DV(40,40),IPREF,JPREF

```

```

1/VAR/  U(40,40),V(40,40),P(40,40),T(40,40),PP(40,40)
1/ALL/  IT,JT,NI,NJ,NIM1,NJM1,GREAT
1/GEOM/ INDCOS,X(32),Y(32),DXEP(32),DXPW(32),DYNP(32),DYPS(32),
1      SNS(32),SEW(32),XU(32),YV(32),R(32),RV(32)
1/FLUPR/URFVIS,VISCOS,DENSIT,PRANDT,DEN(40,40),VIS(40,40),
1      GAMH(40,40)
1/COEF/ AP(40,40),AN(40,40),AS(40,40),AE(40,40),AW(40,40),
1      SU(40,40),SP(40,40)
C *****
C CHAPTER 1 1 1 1 ASSEMBLY OF COEFFICIENTS 1 1 1 1 1 1
C *****
C
DO 100 I=2,NIM1
DO 101 J=3,NJM1
C
C ... COMPUTE AREAS AND VOLUMES
C
AREAN=RCV(J+1)*SEW(I)
AREAS=RCV(J)*SEW(I)
AREAEW=RV(J)*SNSV(J)
VOL=RV(J)*SEW(I)*SNSV(J)
C
C ... CALCULATE CONVECTION COEFFICIENTS
C
GN=0.5*(DEN(I,J+1)+DEN(I,J))*V(I,J+1)
GP=0.5*(DEN(I,J)+DEN(I,J-1))*V(I,J)
GS=0.5*(DEN(I,J-1)+DEN(I,J-2))*V(I,J-1)
GE=0.5*(DEN(I+1,J)+DEN(I,J))*U(I+1,J)
GSE=0.5*(DEN(I,J-1)+DEN(I+1,J-1))*U(I+1,J-1)
GW=0.5*(DEN(I,J-1)+DEN(I-1,J-1))*U(I,J-1)
CN=0.5*(GN+GP)*AREAN
CS=0.5*(GP+GS)*AREAS
CE=0.5*(GE+GSE)*AREAEW
CW=0.5*(GW+GSW)*AREAEW
C
C ... CALCULATE DIFFUSION COEFFICIENTS
C
VISE=0.25*(VIS(I,J)+VIS(I+1,J)+VIS(I,J-1)+VIS(I+1,J-1))
VISW=0.25*(VIS(I,J)+VIS(I-1,J)+VIS(I,J-1)+VIS(I-1,J-1))
DN=VIS(I,J)*AREAN/DYNPV(J)
DE=VISE*AREAEW/DXEP(I)
DS=VIS(I,J-1)*AREAS/DYPSV(J)
DW=VISW*AREAEW/DXPW(I)
C
C ... COMPUTE COEFFICIENTS OF SOURCE TERMS
C
SMP=CN-CS+CE-CW
CP=AMAX1(0.0,SMP)
CPO=CP
C
C ... ASSEMBLE MAIN COEFFICIENTS
C
AN(I,J)=AMAX1(ABS(0.5*CN),DN)-0.5*CN
AS(I,J)=AMAX1(ABS(0.5*CS),DS)+0.5*CS
AE(I,J)=AMAX1(ABS(0.5*CE),DE)-0.5*CE
AW(I,J)=AMAX1(ABS(0.5*CW),DW)+0.5*CW

```

```

DV(I,J)=0.5*(AREAN+AREAS)
SU(I,J)=CPO*V(I,J)+DV(I,J)*(P(I,J-1)-P(I,J))
SP(I,J)=-CP
IF(INDCOS.EQ.2)SP(I,J)=SP(I,J)-VIS(I,J)*VOL/RV(J)**2
101 CONTINUE
100 CONTINUE
C
C *****
C CHAPTER 2 2 2 2 PROBLEM MODIFICATIONS 2 2 2 2 2 2
C *****
C
CALL MODV
C
C *****
C CHAPTER 3 FINAL COEFF. ASSEMBLY AND RESIDUAL SOURCE CALCULATION
C *****
C
RESORV=0.0
DO 300 I=2,NIM1
DO 301 J=3,NJM1
AP(I,J)=AN(I,J)+AS(I,J)+AE(I,J)+AW(I,J)-SP(I,J)
DV(I,J)=DV(I,J)/AP(I,J)
RESOR=AN(I,J)*V(I,J+1)+AS(I,J)*V(I,J-1)+AE(I,J)*V(I+1,J)
1 +AW(I,J)*V(I-1,J)-AP(I,J)*V(I,J)+SU(I,J)
VOL=R(J)*SEW(I)*SNS(J)
SORVOL=GREAT*VOL
IF(-SP(I,J).GT.0.5*SORVOL) RESOR=RESOR/SORVOL
RESORV=RESORV+ABS(RESOR)
C
C ... UNDER-RELAXATION PROCEDURES
C
AP(I,J)=AP(I,J)/URFV
SU(I,J)=SU(I,J)+(1.-URFV)*AP(I,J)*V(I,J)
DV(I,J)=DV(I,J)*URFV
301 CONTINUE
300 CONTINUE
DO 400 N=1,NSWPV
400 CALL LISOLV(2,3,NI,NJ,IT,JT,V)
RETURN
END
C
SUBROUTINE CALCP
C
C *****
C CHAPTER 0 0 0 0 0 PRELIMINARIES 0 0 0 0 0 0
C *****
C
COMMON
1/PCOR/ RESORM,NSWPP,URFP,DU(40,40),DV(40,40),IPREF,JPREF
1/VAR/ U(40,40),V(40,40),P(40,40),T(40,40),PP(40,40)
1/ALL/ IT,JT,NI,NJ,NIM1,NJM1,GREAT
1/GEOM/ INDCOS,X(32),Y(32),DXEP(32),DXPW(32),DYNP(32),DYPS(32),
1 SNS(32),SEW(32),XU(32),YV(32),R(32),RV(32)
1/FLUPR/URFVIS,VISCOS,DENSIT,PRANDT,DEN(40,40),VIS(40,40),
1 GAMH(40,40)

```

```

1/COEF/ AP(40,40),AN(40,40),AS(40,40),AE(40,40),AW(40,40),
1      SU(40,40),SP(40,40)
RESORM=0.0

C
C *****
C CHAPTER 1 1 1 ASSEMBLY OF COEFFICIENTS 1 1 1 1 1
C *****
C
DO 100 I=2,NIM1
DO 101 J=2,NJM1

C
C ... CALCULATE AREAS AND VOLUMES
C
AREAN=RV(J+1)*SEW(I)
AREAS=RV(J)*SEW(I)
AREAEW=R(J)*SNS(J)
VOL=R(J)*SNS(J)*SEW(I)

C
C ... CALCULATE COEFFICIENTS
C
DENN=0.5*(DEN(I,J)+DEN(I,J+1))
DENS=0.5*(DEN(I,J)+DEN(I,J-1))
DENE=0.5*(DEN(I,J)+DEN(I+1,J))
DENW=0.5*(DEN(I,J)+DEN(I-1,J))
AN(I,J)=DENN*AREAN*DV(I,J+1)
AS(I,J)=DENS*AREAS*DV(I,J)
AE(I,J)=DENE*AREAEW*DU(I+1,J)
AW(I,J)=DENW*AREAEW*DU(I,J)

C
C ... CALCULATE SOURCE TERMS
C
CN=DENN*V(I,J+1)*AREAN
CS=DENS*V(I,J)*AREAS
CE=DENE*U(I+1,J)*AREAEW
CW=DENW*U(I,J)*AREAEW
SMP=CN-CS+CE-CW
SP(I,J)=0.0
SU(I,J)=-SMP

C
C ... COMPUTE SUM OF ABSOLUTE MASS SOURCES
C
RESORM=RESORM+ABS(SMP)
101 CONTINUE
100 CONTINUE

C
C *****
C CHAPTER 2 2 2 PROBLEM MODIFICATIONS 2 2 2 2 2
C *****
C
CALL MODP

C
C *****
C CHAPTER 3 3 3 FINAL COEFFICIENT ASSEMBLY 3 3 3 3 3
C *****

```

```

C
C
DO 300 I=2,NIM1
DO 301 J=2,NJM1
301 AP(I,J)=AN(I,J)+AS(I,J)+AE(I,J)+AW(I,J)-SP(I,J)
300 CONTINUE
C
C
*****
C CHAPTER 4 4 SOLUTION OF DIFFERENCE EQUATIONS 4 4 4
C *****
C
DO 400 N=1,NSWPP
400 CALL LISOLV(2,2,NI,NJ,IT,JT,PP)
C
C
*****
C CHAPTER 5 5 5 5 CORRECT VELOCITIES AND PRESSURE 5 5 5 5
C *****
C
... VELOCITIES
C
DO 500 I=2,NIM1
DO 501 J=2,NJM1
IF(I.NE.2)U(I,J)=U(I,J)+DU(I,J)*(PP(I-1,J)-PP(I,J))
IF(J.NE.2)V(I,J)=V(I,J)+DV(I,J)*(PP(I,J-1)-PP(I,J))
501 CONTINUE
500 CONTINUE
C
... PRESSURES (WITH PROVISIONS FOR UNDER RELAXATION)
C
PPREF=PP(IPREF,JPREF)
DO 502 I=2,NIM1
DO 503 J=2,NJM1
P(I,J)=P(I,J)+URFP*(PP(I,J)-PPREF)
PP(I,J)=O.O
503 CONTINUE
502 CONTINUE
RETURN
END
C
SUBROUTINE CALCT
C
*****
C CHAPTER 0 0 0 0 0 PRELIMINARIES 0 0 0 0 0 0 0 0
C *****
C
COMMON
1/TEMP/ RESORT,NSWPT,URFT
1/VAR/ U(40,40),V(40,40),P(40,40),T(40,40),PP(40,40)
1/ALL/ IT,JT,NI,NJ,NIM1,NJM1,GREAT
1/GEOM/ INDCOS,X(32),Y(32),DXEP(32),DXPW(32),DYNP(32),DYPS(32),
1 SNS(32),SEW(32),XU(32),YV(32),R(32),RV(32)
1/FLUPR/URFVIS,VISCOS,DENSIT,PRANDT,DEN(40,40),VIS(40,40),
1 GAMH(40,40)

```

```

1/COEF/ AP(40,40),AN(40,40),AS(40,40),AE(40,40),AW(40,40),
1 SU(40,40),SP(40,40)
C *****
C CHAPTER 1 1 1 ASSEMBLY OF COEFFICIENTS 1 1 1
C *****
C
C DO 100 I=2,NIM1
C DO 101 J=2,NJM1
C
C ... COMPUTE AREAS AND VOLUME
C
C AREAN=RV(J+1)*SEW(I)
C AREAS=RV(J)*SEW(I)
C AREAEW=R(J)*SNS(J)
C VOL=R(J)*SNS(J)*SEW(I)
C
C ... CALCULATE CONVECTION COEFFICIENTS
C
C GN=0.5*(DEN(I,J)+DEN(I,J+1))*V(I,J+1)
C GS=0.5*(DEN(I,J)+DEN(I,J-1))*V(I,J)
C GE=0.5*(DEN(I,J)+DEN(I+1,J))*U(I+1,J)
C GW=0.5*(DEN(I,J)+DEN(I-1,J))*U(I,J)
C CN=GN*AREAN
C CS=GS*AREAS
C CE=GE*AREAEW
C CW=GW*AREAEW
C
C ... CALCULATE DIFFUSION COEFFICIENTS
C
C GAMN=0.5*(GAMH(I,J)+GAMH(I,J+1))
C GAMS=0.5*(GAMH(I,J)+GAMH(I,J-1))
C GAME=0.5*(GAMH(I,J)+GAMH(I+1,J))
C GAMW=0.5*(GAMH(I,J)+GAMH(I-1,J))
C DN=GAMN*AREAN/DYNP(J)
C DS=GAMS*AREAS/DYPS(J)
C DE=GAME*AREAEW/DXEP(I)
C DW=GAMW*AREAEW/DXPW(I)
C
C ... SOURCE TERMS
C
C SMP=CN-CS+CE-CW
C CP=AMAX1(0.0,SMP)
C CPO=CP
C
C ... ASSEMBLE MAIN COEFFICIENTS
C
C AN(I,J)=AMAX1(ABS(0.5*CN),DN)-0.5*CN
C AS(I,J)=AMAX1(ABS(0.5*CS),DS)+0.5*CS
C AE(I,J)=AMAX1(ABS(0.5*CE),DE)-0.5*CE
C AW(I,J)=AMAX1(ABS(0.5*CW),DW)+0.5*CW
C SU(I,J)=CPO*T(I,J)
C SP(I,J)=-CP
101 CONTINUE
100 CONTINUE
C
C *****

```

```

C      CHAPTER 2 2 2 PROBLEM MODIFICATIONS 2 2 2 2
C      *****
C
C      CALL MODT
C
C      *****
C      CHAPTER 3 FINAL COEFF. ASSEMBLY AND RESIDUAL SOURCE CALCULATION
C      *****
C
C      RESORT=0.0
C      DO 300 I=2,NIM1
C      DO 301 J=2,NJM1
C      AP(I,J)=AN(I,J)+AS(I,J)+AE(I,J)+AW(I,J)-SP(I,J)
C      RESOR=AN(I,J)*T(I,J+1)+AS(I,J)*T(I,J-1)+AE(I,J)*T(I+1,J)
C      1 +AW(I,J)*T(I-1,J)-AP(I,J)*T(I,J)+SU(I,J)
C      VOL=R(J)*SEW(I)*SNS(J)
C      SORVOL=GREAT*VOL
C      IF(-SP(I,J).GT.0.5*SORVOL) RESOR=RESOR/SORVOL
C      RESORT=RESORT+ABS(RESOR)
C
C      ... UNDER-RELAXATION
C
C      AP(I,J)=AP(I,J)/URFT
C      SU(I,J)=SU(I,J)+(1.-URFT)*AP(I,J)*T(I,J)
C      301 CONTINUE
C      300 CONTINUE
C
C      *****
C      CHAPTER 4 4 4 SOLUTION OF DIFFERENCE EQUATION 4 4 4
C      *****
C
C      DO 400 N=1,NSWPT
C      400 CALL LISOLV(2,2,NI,NJ,IT,JT,T)
C      RETURN
C      END
C
C      SUBROUTINE LISOLV(ISTART,JSTART,NI,NJ,IT,JT,PHI)
C
C      *****
C      CHAPTER 0 0 0 0 PRELIMINARIES 0 0 0 0 0
C      *****
C
C      DIMENSION PHI(IT,JT),A(32),B(32),C(32),D(32)
C      COMMON
C      1/COEF/ AP(40,40),AN(40,40),AS(40,40),AE(40,40),AW(40,40),
C      1 SU(40,40),SP(40,40)
C      NIM1=NI-1
C      NJM1=NJ-1
C      JSTM1=JSTART-1
C      A(JSTM1)=0.0
C
C      ... THIS LOOP SETS UNDERFLOW VALUES TO ZERO

```

```

C
DO 1 I=ISTART,NIM1
DO 1 J=JSTART,NJM1
  IF (ABS(AE(I,J)).LT.1.E-10) AE(I,J)=0.0
  IF (ABS(AW(I,J)).LT.1.E-10) AW(I,J)=0.0
  IF (ABS(AN(I,J)).LT.1.E-10) AN(I,J)=0.0
  IF (ABS(AS(I,J)).LT.1.E-10) AS(I,J)=0.0
  IF (ABS(PHI(I,J)).LT.1.E-10) PHI(I,J)=0.0
1 CONTINUE
C
C ... COMMENCE W-E SWEEP
C
DO 100 I=ISTART,NIM1
C(JSTM1)=PHI(I,JSTM1)
C
C ... COMMENCE S-N SWEEP
C
DO 101 J=JSTART,NJM1
C
C ... ASSEMBLE TDMA COEFFICIENTS
C
A(J)=AN(I,J)
B(J)=AS(I,J)
C(J)=AE(I,J)*PHI(I+1,J)+AW(I,J)*PHI(I-1,J)+SU(I,J)
D(J)=AP(I,J)
C
C ... CALCULATE COEFFICIENTS OF RECURRENCE FORMULA
C
C ? TERM=1./(D(J)-B(J)*A(J-1))
TERM=0.0
DMBMA=D(J)-B(J)*A(J-1)
IF (ABS(DMBMA).GT.1.E-07) TERM=1./DMBMA
A(J)=A(J)*TERM
IF (ABS(C(J-1)).LT.1.E-10) C(J-1)=0.0
101 C(J)=(C(J)+B(J)*C(J-1))*TERM
C
C ... OBTAIN NEW PHI'S
C
DO 102 JJ=JSTART,NJM1
J=NJ+JSTM1-JJ
IF (ABS(PHI(I,J+1)).LT.1.E-10) PHI(I,J+1)=0.0
102 PHI(I,J)=A(J)*PHI(I,J+1)+C(J)
100 CONTINUE
RETURN
END
C
SUBROUTINE PRINT(ISTART,JSTART,NI,NJ,IT,JT,X,Y,PHI,HEAD)
C
DIMENSION PHI(IT,JT),X(IT),Y(JT),HEAD(6),STORE(50)
DIMENSION F(7),F4(11)
DATA F/4H(1H,4H,A6,.4HI3,4H11I,4H10,4H7X,
14HA6) /
DATA F4/4H 1I,4H 2I,4H 3I,4H 4I,4H 5I,4H 6I,
1 4H 7I,4H 8I,4H 9I,4H10I,4H11I /
DATA HI,HY/4H I =,4HY = /
LP = 6

```



```

      ISKIP=1
      JSKIP=1
      WRITE(LP,110)HEAD
      ISTA=ISTART-12
100  CONTINUE
C
      ISTA=ISTA+12
      IEND=ISTA+11
      IEND=MINO(NI,IEND)
      F(4)=F4(IEND-ISTA)
      WRITE(LP,F) HI, (I,I=ISTA,IEND,ISKIP), HY
      WRITE(LP,112)
      DO 101 JJ=JSTART,NJ,JSKIP
      IF (X(I).LT.XMIN) XMIN = X(I)
      J=JSTART+NJ-JJ
      DO 120 I=ISTA,IEND
      A=PHI(I,J)
      IF(ABS(A).LT.1.E-20)A=0.0
120  STORE(I)=A
101  WRITE(LP,113) J,(STORE(I),I=ISTA,IEND,ISKIP),Y(J)
      WRITE(LP,114)(X(I),I=ISTA,IEND,ISKIP)
      WRITE(LP,115)
C
      IF (IEND.LT.NI) GOTO 100
      RETURN
110  FORMAT(//1H ,28(2H*-),7X,A5,7X,28(2H-*))
111  FORMAT(//1H ,6H I = ,I3,11I10,7X,' Y = ')
112  FORMAT(3H J)
113  FORMAT(1H ,I3,1P12E10.2,OPF7.3)
114  FORMAT(6H X= ,F7.3,11F10.3)
115  FORMAT(//)
      END
C
      SUBROUTINE PLOT(X,IDIM,IMAX,XAXIS,Y,JDIM,JMAX,YAXES,SYMBOL,LP,
1      ID)
C
C COMMENT ***** COMMENT
C
C      SUBROUTINE FOR PLOTTING J CURVES OF Y(I,J) AGAINST X(I).
C
C      X AND Y ARE ASSUMED TO BE IN ANY RANGE EXCEPT THAT NEGATIVE
C      NEGATIVE VALUES ARE PLOTTED AS ZERO.
C
C      X AND Y ARE SCALED TO THE RANGE 0. TO 1. BY DIVISION BY THE
C      MAXIMUM, WHICH IS PRINTED AS WELL.
C
C      IDIM IS THE VARIABLE DIMENSION FOR X.
C
C      IMAX IS THE NUMBER OF X VALUES.
C
C      XAXIS STORES THE NAME OF THE X-AXIS.
C
C      JDIM IS THE VARIABLE DIMENSION FOR Y.
C
C      JMAX IS THE NUMBER OF CURVES TO BE PLOTTED, (UP TO 10).
C

```

```

C          THE ARRAY YAXIS(J) STORES THE NAMES OF THE CURVES.          C
C
C          THE ARRAY SYMBOL(J) STORES THE SINGLE CHARACTERS USED FOR    C
C          PLOTTING.                                                    C
C
COMMENT ***** COMMENT
C
C ... DIMENSION NEEDED ARRAYS FOR PLOT SUBROUTINE
C
      DIMENSION X(IDIM),Y(JDIM,IDIM),A(101),SYMBOL(ID)
      CHARACTER*12 YAXES(JDIM),XAXIS
      DATA DOT,CROSS,BLANK/1H.,1H+,1H /
C
C ... VARIABLES USED FOR THE COORDINATE-AXISES
C
C ... SCALING X ARRAY TO THE RANGE 0 TO 50
C
      XMIN = 1.OE30
      XMAX = 1.E-30
      DO 1 I = 1,IMAX
      IF (X(I).GT.XMAX) XMAX = X(I)
      IF (X(I).LT.XMIN) XMIN = X(I)
1     CONTINUE
      XM = 100./(XMAX-XMIN)
      XN = -XMIN*XM
      DO 2 I = 1,IMAX
      X(I) = X(I)*XM+XN
      IF (X(I).LT.O.) X(I) = O.
2     CONTINUE
C
C ... SCALING Y ARRAY TO THE RANGE 0 TO 100
C
      YMIN = 1.OE30
      YMAX = 1.OE-30
      DO 3 J = 1,JMAX
      DO 3 I = 1,IMAX
      IF (Y(J,I).GT.YMAX) YMAX = Y(J,I)
      IF (Y(J,I).LT.YMIN) YMIN=Y(J,I)
3     CONTINUE
      YM = 50./(YMAX-YMIN)
      YN = -YMIN*YM
      DO 4 J = 1,JMAX
      DO 4 I = 1,IMAX
C
C ... Y SCALING
C
      Y(J,I) = Y(J,I)*YM+YN
      IF (Y(J,I).LT.O.) Y(J,I) = O.
4     CONTINUE
C
C ... IDENTIFYING THE VARIOUS CURVES TO BE PLOTTED
C
      WRITE(LP,103) XAXIS
      WRITE(LP,100) (YAXES(I),I = 1,JMAX)
      WRITE(LP,106) (SYMBOL(I),I = 1,JMAX)

```

```

WRITE(LP,102) (YMAX,I=1,JMAX)
DO 5 I = 1,11
5  A(I) = (XMAX-XMIN)*(I-1)/10.
WRITE(LP,101) (A(I),I = 1,11)
C
C ... MAIN LOOP. EACH PASS PRODUCES AN X-CONSTANT LINE.
C
DO 40 II = 1,51
I = 51-II+1
IF (I.EQ.1.OR.I.EQ.51) GOTO 32
GOTO 33
C
C ... ALLOCATE . OR + MARK ON THE Y-AXIS
C
32 DO 30 K = 1,101
30  A(K) = DOT
DO 31 K = 11,101,10
31  A(K) = CROSS
C
C ... ALLOCATE . OR + MARK ON THE X-AXIS, ALSO THE APPROPRIATE
C ... X VALUE.
C
33  A(1) = DOT
A(101) = DOT
K = II-1
46  K = K-5
IF (K) 48,47,46
47  A(1) = CROSS
A(101) = CROSS
48  YL = YMAX-0.02*(YMAX-YMIN)*(II-1)
C
C ... CHECK IF ANY Y(X(I)) VALUE LIES ON THIS X-CONSTANT LINE
C ... IF YES GOTO 41, OTHERWISE CHECK FO OTHERS ON Y-CONSTANT LINE.
C
DO 43 K = 1,IMAX
DO 44 J = 1,JMAX
IFIX = Y(J,K)+1.5
IF(IFIX-I)44,41,44
44  CONTINUE
IF (J.EQ.JMAX+1) GOTO 43
C
C ... LOCATE Y(X(I))
C
41  NY = X(K)+1.5
A(NY) = SYMBOL(J)
43  CONTINUE
C
C ... PRINT X-CONSTANT LINE
C
WRITE(LP,105) YL,(A(K),K = 1,101),YL
C
C ... PUTTING BLANKS INTO X-CONSTANT LINE
C
DO 49 K = 1,101
49  A(K) = BLANK
40  CONTINUE

```

```
DO 50 I = 1,11
A(I) = 0.1*(XMAX-XMIN)*(I-1)
WRITE(LP,104) (A(I),I = 1,11)
DO 60 I = 1,IMAX
X(I) = (X(I)-XN)/XM
DO 60 J = 1,JMAX
60 Y(J,I) = (Y(J,I)-YN)/YM
RETURN
C
C ... FORMAT STATEMENTS
C
100 FORMAT(11H Y-AXES ARE,5X,10(1X,A12))
101 FORMAT(//,9X,11F10.6)
102 FORMAT(15H MAXIMUM VALUES, 10E11.3)
103 FORMAT(///11H X-AXIS IS ,A12)
104 FORMAT(9X,11F10.6)
105 FORMAT(3H Y=,F6.2,3X,101A1,F6.2)
106 FORMAT(7H SYMBOL,11X,10(1X,A10))
C
C ... END OF SUBROUTINE PLOT
C
C
C
C
C *****
C          END OF THE TEACHL CODE
C *****
C
```

VITA 2

Matthew Jess Maxwell

Candidate for the Degree of

Master of Science

Thesis: COMPUTER SIMULATION OF LAMINAR FORCED CONVECTIVE HEAT TRANSFER
IN THE ENTRANCE REGION OF A STRAIGHT CHANNEL FOR CONSTANT- AND
VARIABLE-PROPERTY GASES

Major Field: Mechanical Engineering

Biographical:

Personal Data: Born in Augusta, Georgia, July 19, 1961, the son of
Mr. and Mrs. Jess B. Maxwell.

Education: Graduated from Putnam City High School, Oklahoma City,
Oklahoma, May, 1979; received the Bachelor of Science in
Mechanical Engineering degree from Oklahoma State University,
May, 1983; completed the requirements for the Master of
Science degree at Oklahoma State University, May, 1984.

Professional Experience: Manufacturing and Engineering Engineer,
Gardner Denver of Cooper Industries, Mesquite, Texas, 1981;
Well Site Data Transmissions, Schlumberger Well Services,
Dallas, Texas, 1982; Teaching Assistant, Oklahoma State
University, Stillwater, Oklahoma, 1982-1983; registered
Engineer Intern (EIT), State of Oklahoma.

Professional Societies: American Society of Mechanical Engineers;
National Society of Professional Engineers.